

Robust Phase Retrieval and Super-Resolution from One Bit Coded Diffraction Patterns.

YOUSSEF MROUEH^{†,★}

[†] *CBCL, McGovern Institute, [‡]CSAIL, MIT, USA.*

[★] *LCSL, Massachusetts Institute of Technology and Istituto Italiano di Tecnologia.*

ymroueh@mit.edu

September 7, 2021

Abstract

In this paper we study a realistic setup for phase retrieval, where the signal of interest is modulated or masked and then for each modulation or mask a diffraction pattern is collected, producing a coded diffraction pattern (CDP) [CLM13]. We are interested in the setup where the resolution of the collected CDP is limited by the Fraunhofer diffraction limit of the imaging system. We investigate a novel approach based on a geometric quantization scheme of phase-less linear measurements into (one-bit) coded diffraction patterns, and a corresponding recovery scheme. The key novelty in this approach consists in comparing pairs of coded diffractions patterns across frequencies: the one bit measurements obtained rely on the order statistics of the un-quantized measurements rather than their values. This results in a robust phase recovery, and unlike currently available methods, allows to efficiently perform phase recovery from measurements affected by severe (possibly unknown) non linear, rank preserving perturbations, such as distortions. Another important feature of this approach consists in the fact that it enables also super-resolution and blind-deconvolution, beyond the diffraction limit of a given imaging system.

1 Introduction

1.1 The Phase Retrieval Problem and the Diffraction Limit

The problem of phase retrieval is ubiquitous in many areas of imaging science and engineering, where we are able to measure only magnitude of measurements. The phase recovery problem can be modeled as the problem of reconstructing a n -dimensional complex vector x_0 given only the magnitude of m phase-less linear measurements. Such a problem arises for example in X-ray crystallography [Har93, Lea08], diffraction imaging [BDP⁺07, Rod08] or microscopy [MISE08], where one can only measure the intensities of the incoming waves, and wishes to recover the lost phase in order to be able to reconstruct the desired object. Formally speaking for a given vector $x_0 \in \mathbb{C}^n$ (without loss of generality we assume n to be even), we wish to measure $\langle a_k, x \rangle$, but the only available information is of the form:

$$b_k = \theta(|\langle a_k, x \rangle|^2), k = 1 \dots m, \quad (1)$$

where a_k is a set of sampling vector in \mathbb{C}^n , and θ models possibly unknown non linear perturbations of the values: distortion and exponential noise for instance.

Recovering signals from the modulus of their Fourier transform is at the core of the phase retrieval problem. For instance in coherent X-ray crystallography [Lea08], speckle imaging in astronomy [Fri66], in microscopy [Gus00] or more broadly in Fourier optics it follows from the Fraunhofer diffraction principle that the optical field at the detector can be approximated by the Fourier transform of the sensed object. Since light detectors can measure only intensities of the incoming waves the problem is therefore to recover the discrete signal $x_0 \in \mathbb{C}^n$ from measurements of the type:

$$b_k = \theta \left(\left| \sum_{j=1}^n x_0[j] e^{-i2\pi(j-1)\frac{(k-1)}{n}} \right|^2 \right), \quad k \in \Omega, \quad \Omega \subseteq [1, n] \quad (2)$$

where Ω represents a set of sampled frequencies, and θ a possibly unknown non-linearity. When compared to (1) we note that in (2) a_k correspond to a set of sampled complex sinusoids. When $\Omega = [1, n]$, we have the full knowledge of the modulus of the Fourier series decomposition of the signal of interest on whole ranges of frequencies. In practice due to the Fraunhofer diffraction limit we are able to measure intensities of the Fourier transform within a range of frequencies below the so called cut-off frequency f_c . Hence the information we have available about x_0 is a sample of the lower end of its power spectra in the form of the lowest $2f_c + 1$ modulus of the Fourier series coefficients (f_c is an integer).

For instance in microscopy imaging with coherent illumination the object of interest is diffracted through a lens. The lens is characterized by its Point Spread Function (PSF) h , and the cut-off frequency $f_c = \frac{2\pi NA}{\nu}$, where NA is the numerical aperture of the lens and ν is the wavelength of the illumination light. Let \hat{h}, \hat{x}_0 be the Fourier transform of the PSF and the signal x_0 respectively, for continuous signals we know that:

$$\hat{h}(w) = 0 \quad \text{for } |w| > f_c.$$

Hence we measure the modulus of the Fourier transform of $x_0 \star h$ rather than x_0 , where \star denotes the discrete convolution operation. If we set $\theta = \theta_h$, where

$$\theta_h \left(\left| \sum_{j=1}^n x_0[j] e^{-i2\pi(j-1)\frac{(k-1)}{n}} \right|^2 \right) := \left| \sum_{j=1}^n (x_0 \star h)[j] e^{-i2\pi(j-1)\frac{(k-1)}{n}} \right|^2,$$

equation (2) becomes (with some abuse of notation, in re-indexing k between $-\frac{n}{2}$ and $\frac{n}{2} - 1$):

$$b_k = |\hat{h}_k|^2 |\hat{x}_0_k|^2 \quad k \in \llbracket -f_c, f_c \rrbracket \text{ and } b_k = 0 \text{ elsewhere.} \quad (3)$$

It follows from equation (3), that in addition to the missing phase problem we are facing a super-resolution problem since the high frequency content of the signal is also lost due to the physical resolution limit induced by the cut-off frequency f_c (See for e.g. [Gus00]).

This paper answers the following questions:

1. *Robust recovery: Is it possible to robustly recover the missing phase from the power spectra of a signal x_0 that is undergoing severe unknown non linear distortions or a stochastic noise?*
2. *Phase Recovery, Super-Resolution, and Blind deconvolution: Is it possible to recover the signal from the lower end of its power spectra? In other words is it possible to super-resolve the signal beyond the diffraction limit of a given optical system even if the PSF of that system was unknown (blind deconvolution)?*

Notations: \star represents a convolution, and \odot the Hadamard product (component-wise product). For $z \in \mathbb{C}$, $|z|^2$ is squared complex modulus of z . For $a, a' \in \mathbb{C}^n$, $\langle a, a' \rangle$ is the complex dot product in \mathbb{C}^n . For $a \in \mathbb{C}^n$, a^* is the complex conjugate of a , $\|a\|_2$ is the norm 2 of a and \cdot . Let A a complex hermitian matrix in \mathbb{C}^n , $\|A\|_F$ denotes the Frobenius norm of A , $\|A\|$ demotes the operator norm of A , $Tr(A)$ denotes the trace of A . Throughout the paper, we denote by c, C positive absolute constants whose values may change from instance to instance.

1.2 Phase Retrieval: Previous Work

As mentioned in the introduction the set of sampling vectors we are interested in, is the set of complex sinusoids. Before tackling the Fourier based sampling we turn to the setting pioneered by [CSV11] where the set of sampling vectors is randomized, i.e we consider a set of independent measurements defined by independent and identically distributed Complex Gaussian sensing vectors,

$$a_i \in \mathbb{C}^n, \quad a_i \sim \mathcal{N}(0, \frac{1}{2}I_n) + i\mathcal{N}(0, \frac{1}{2}I_n), \quad i = 1 \dots m. \quad (4)$$

The (noiseless) phase recovery problem is defined as follow.

Definition 1 (Phase-less Sensing and Phase Recovery). *Suppose phase-less sensing measurements*

$$b_i = |\langle a_i, x_0 \rangle|^2 \in \mathbb{R}_+, \quad i = 1 \dots m, \quad (5)$$

are given for $x_0 \in \mathbb{C}^n$, where a_i , $i = 1, \dots, m$ are random vectors as in (4). The phase recovery problem is

$$\text{find } x, \quad \text{subject to } |\langle a_i, x \rangle|^2 = b_i, \quad i = 1 \dots m. \quad (6)$$

The above problem is non convex and in the following we recall recent approaches to provably and efficiently recover x_0 from a finite number of measurements.

SDP (Convex) Relaxation and PhaseLift. The PhaseLift approach [CSV11] stems from the observation that $|\langle a_i, x \rangle|^2 = Tr(a_i a_i^* x x^*)$, so that if we let $X = x x^*$, Problem 6 can be written as,

$$\text{find } X, \quad \text{subject to } Tr(a_i a_i^* X) = b_i, \quad i = 1 \dots m, \quad X \succeq 0, \quad rank(X) = 1. \quad (7)$$

While the above formulation is still non convex (and in fact combinatorially hard because of the rank constraint), a convex relaxation can be obtained noting that Problem 7 can be written as a rank minimization problem over the positive semi-definite cone,

$$\min_X rank(X), \quad \text{subject to } Tr(a_i a_i^* X) = b_i, \quad i = 1 \dots m, \quad X \succeq 0, \quad (8)$$

and then considering the trace as a surrogate for the rank [CSV11],

$$\min_X Tr(X), \quad \text{subject to } Tr(a_i a_i^* X) = b_i, \quad i = 1 \dots m, \quad X \succeq 0. \quad (9)$$

Indeed, the above problem is convex and can be solved via semidefinite programming (SDP). Intestingly, a different relaxation is obtained in [DH12] by ignoring the rank constraint in Problem 7. The results in [CSV11, DH12] show that, with high probability, the solution \hat{X}_m obtained via either one of the above relaxations can recover x_0 exactly i.e. $\hat{X}_m = x_0 x_0^*$, as soon as $m \geq cn \log n$. In fact, the latter requirement can be further improved to $m \geq cn$ [CL12]. While powerful, the convex relaxation approach incur in cumbersome computations, and in practice non convex approaches based on greedy alternating minimization (AM) [GS72, Fie82, GL84] are often used.

The convergence properties of the latter methods depend heavily on the initialization and only recently [NJS13] they have been shown to globally converge (with high probability) if provided with a suitable initialization.

Phase Retrieval via Suitably Initialized Alternating Minimization. Let A be the matrix defined by m sensing vectors as in (4) and $B = \text{Diag}(\sqrt{b})$, where b is the vector of measurements as in (5). Then

$$Ax_0 = Bu_0$$

for $u_0 = Ph(Ax_0)$ with $Ph(z) = \left(\frac{z_1}{|z_1|}, \dots, \frac{z_m}{|z_m|} \right)$, $z \in \mathbb{C}^m$. The above equality suggests the following natural approach to recover (x_0, u_0) ,

$$\min_{x,u} \|Ax - Bu\|^2, \quad \text{subject to } |u_i| = 1, \quad i = 1 \dots m, \quad (10)$$

The above problem is not convex because of the constraint on u and the AM approach consists in optimizing u , for a given x , and then optimizing x for a given u . It is easy to see that for a given x , the optimal u is simply $u = Ph(Ax)$, and, for a given u , the optimal x is the solution of a least square problem. The key result in [NJS13] shows that if such an iteration is initialized with the maximum eigenvector of the matrix

$$\hat{C}_m = \frac{1}{m} \sum_{i=1}^m b_i a_i a_i^* \quad (11)$$

then the solution of the alternating minimization x_{t_0} globally converges (with high probability) to the true vector x_0 . Throughout this paper we call this initialization *SubExp* initialization. Moreover for a given accuracy ϵ , $0 < \epsilon < 1$, if

$$m \geq c(n(\log^3 n + \log \frac{1}{\epsilon} \log \log \frac{1}{\epsilon})), \quad (12)$$

then $\|x_{t_0} - e^{i\phi} x_0\|_2 \leq \epsilon$.

One Bit Phase Retrieval and Greedy Refinements. More recently a new approach for phase retrieval was proposed in [MR13] based on a quantization scheme of severely perturbed phase-less linear measurements. Assume we observe pairs of independent phase-less measurements:

$$(b_i^1, b_i^2) = (\theta(|\langle a_i^1, x_0 \rangle|^2), \theta(|\langle a_i^2, x_0 \rangle|^2)), \quad i = 1, \dots, m, \quad (13)$$

where (a_i^1, a_i^2) are independent sensing vectors as in (4) and θ is a *possibly unknown* rank preserving transformation. In particular θ models a distortion, e.g. $\theta(s) = \tanh(\alpha s)$, $\alpha \in \mathbb{R}_+$, or an additive noise $\theta(s) = s + \nu$, where ν is a stochastic noise, such as an exponential noise. The recovery problem from severely perturbed intensity values seems hopeless, and indeed the key in this approach is a quantization scheme based on comparing pairs of phase-less measurements. More precisely for each pair b_i^1, b_i^2 of measurements of the form (13) we define

$$y_i \in \{-1, 1\} \quad y_i = \text{sign}(b_i^1 - b_i^2), \quad i = 1 \dots m.$$

The one bit phase retrieval problem reduces to a maximum eigenvalue problem induced by the matrix

$$\hat{C}_m = \frac{1}{m} \sum_{i=1}^m y_i (a_i^1 a_i^{1,*} - a_i^2 a_i^{2,*}). \quad (14)$$

In [MR13] it is shown that the expectation of \hat{C}_m satisfies $\mathbb{E}\hat{C}_m = \lambda x_0 x_0^*$, where λ is a suitable constant which depends on θ and plays the role of a signal-to-noise ratio. Moreover for a given accuracy $\epsilon, 0 < \epsilon < 1$, if $O(\frac{n \log n}{\epsilon^2 \lambda})$ pairs of measurements are available, then the solution \hat{x}_m of the above maximum eigenvalue problem satisfies

$$\|\hat{x}_m - x_0 e^{i\phi}\|_2^2 \leq \epsilon,$$

where $\phi \in [0, 2\pi]$ is a global phase. Interestingly authors in [MR13] show that provided with the one-bit retrieval initialization, the solution of the alternating minimization algorithm x_{t_0} globally converges (with high probability) to the true vector x_0 :if

$$m \geq c(n(\log n + \log \frac{1}{\epsilon} \log \log \frac{1}{\epsilon})), \quad (15)$$

then $\|x_{t_0} - e^{i\phi} x_0\|_2 \leq \epsilon$. Hence quantization plays the role of a preconditioning that enhances the sample complexity of the overall alternating minimization.

1.3 Coded Diffraction Patterns and PhaseLift

While the Gaussian measurements setting allow to carry an interesting theory and gives a glimpse on the efficiency of proposed methods in more practical setups, it is of great interest to study the Fourier sampling mentioned in the introduction. A practical setup consists in modulating the signal with multiple structured illuminations for instance, and then measuring multiple diffraction patterns of the modulated signals. The modulation step could be replaced by masking the signal of interest with an appropriate mask. This is indeed an attractive framework to resolve the ambiguity in the phase retrieval problem. Firstly suggested in [Mis73], this technique comes under different names: digital holography [YZ97], ptychography [HKH⁺13], Fourier ptychographic microscopy [ZHY13], etc.. These techniques yield to many successful applications in structured illumination microscopy [Gus00] and more broadly in many linear and non linear Fourier optics applications, where both phase retrieval and super-resolution are achieved via masking or the use of multiple structured illumination modulation. Let $w_\ell \in \mathbb{C}^n, \ell = 1 \dots r$ be the modulating waves (or the masks), we observe the following coded diffraction patterns [CLM13] :

$$b_{\ell,k} = \theta \left(\left| \sum_{j=1}^n x_0[j] w_\ell[j] e^{-i2\pi(j-1)\frac{(k-1)}{n}} \right|^2 \right), \quad k \in \Omega, \quad \Omega \subseteq [1, n], \quad \ell = 1 \dots r. \quad (16)$$

In other words, noting F the Discrete Fourier Transform (DFT) Matrix, $Diag(w)$ the diagonal matrix with the modulation pattern on its diagonal, and $\Omega = [1, n]$ we have:

$$b_\ell = \theta(|F Diag(w_\ell) x_0|^2) \in \mathbb{R}_+^n \quad \ell = 1 \dots r, \quad (17)$$

where θ and the complex modulus act component-wise. In a recent work, for $\theta(z) = z$, and a set of admissible modulations authors in [CLM13] show that an approach similar to Phase-lift allows the exact recovery of the signal with high probability given that:

$$r \geq c \log^4 n,$$

for a fixed numerical constant c .

In [ABFM12, ASBM13] authors introduce another approach to phase retrieval by polarization. In [ASBM13] authors propose a construction of binary masks that ensures phase recovery by polarization. It is shown in [ASBM13] that $O(\log(n))$ binary masks are needed to ensure recovery in the noiseless case.

Indeed with this subset of papers on phase retrieval we don't give justice to a large body of papers on that issue for a succinct review we refer the reader to [CLM13] and references therein.

1.4 This Paper: One Bit Coded Diffraction Patterns

In this paper we are interested in the setting where θ is different from the identity. We restrict our analysis to complex Gaussian modulations. Three settings are of interest:

1. *Noise:*

★ *Additive Stochastic noise:* We observe noisy coded diffraction patterns,

$$b_\ell = |F\text{Diag}(w_\ell)x_0|^2 + \nu_\ell \in \mathbb{R}_+^n \quad \ell = 1 \dots 2r, \quad (18)$$

where ν_ℓ are independent exponential vectors $\text{Exp}(\gamma)$, ($\sigma = \frac{1}{\gamma^2}$).

★ *Poisson Noise:* We observe noisy coded diffraction patterns contaminated with poisson noise,

$$b_\ell = \mathcal{P}_\eta (|F\text{Diag}(w_\ell)x_0|^2) \in \mathbb{R}_+^n \quad \ell = 1 \dots 2r, \quad (19)$$

where \mathcal{P}_η is a component-wise poisson noise : For $z, \eta > 0$, $\mathcal{P}_\eta(z) \sim \text{Poisson}(\frac{z}{\eta})$.

2. *Distortion:* We observe distorted coded diffraction patterns:

$$b_\ell = \tanh(\alpha|F\text{Diag}(w_\ell)x_0|^2) \in \mathbb{R}_+^n \quad \ell = 1 \dots 2r, \alpha > 0, \quad (20)$$

(with some abuse of notations \tanh acts component-wise).

3. *Diffraction Limit/Super-Resolution/Blind deconvolution:* The modulated signal diffracts through a lens characterized by a PSF h and a cut-off frequency f_c . Let H be the Toeplitz matrix associated to h , we observe:

$$b_\ell = |FH\text{Diag}(w_\ell)x_0|^2 \in \mathbb{R}_+^n, \quad \ell = 1 \dots 2r. \quad (21)$$

In this paper we take the point of view of [MR13] and define a quantization scheme for the coded diffraction patterns, by comparing pairs of coded diffraction patterns. Consider pairs of coded diffraction patterns associated to pairs of independent modulations (w_i^1, w_i^2) , where $w_i^1, w_i^2 \sim \mathcal{CN}(0, I_n)$:

$$(b_i^1, b_i^2) = (\theta(|F\text{Diag}(w_i^1)x_0|^2), \theta(|F\text{Diag}(w_i^2)x_0|^2)) \in \mathbb{R}_+^n \times \mathbb{R}_+^n \quad i = 1 \dots r. \quad (22)$$

For each pair (b_i^1, b_i^2) of coded diffraction patterns we define a one bit coded diffraction pattern as:

$$y_i \in \{-1, 1\}^n, \quad y_i = \text{sign}(b_i^1 - b_i^2), i = 1 \dots r. \quad (23)$$

Now the One Bit Phase Retrieval problem consists in finding x_0 from the knowledge of one bit coded diffraction patterns $(y_1 \dots y_r)$. Similarly to One bit phase retrieval from Gaussian measurements we show that the phase retrieval problem from one bit coded diffraction patterns reduces to finding the maximum eigen-vector \hat{x}_r of the matrix \hat{C}_r :

$$\hat{C}_r = \frac{1}{r} \sum_{i=1}^r \left(\text{Diag}(w_i^1)F\text{Diag}(y_i)F^* \text{Diag}(w_i^{1,*}) - \text{Diag}(w_i^2)F\text{Diag}(y_i)F^* \text{Diag}(w_i^{2,*}) \right), \quad (24)$$

Indeed in this paper we show that :

$$\mathbb{E}(\hat{C}_r) = \lambda x_0 x_0^*,$$

where λ depends on θ .

2 Main Results

In the following we give the only assumption we make on θ throughout the paper, and state our main results for the three setups of interest discussed in Section 1.4. As mentioned before, we assume that θ preserves the ranking of the intensities. We shall make one assumption on the non linearity θ ,

$$\lambda = \mathbb{E}(\langle \text{sign}(\theta(E_1) - \theta(E_2)), (E_1 - E_2) \rangle) > 0, \quad (25)$$

where E_1, E_2 are two independently distributed exponential random n -dimensional vectors with mean $\frac{1}{n}$. To see why this assumption is natural, notice that $|F\text{Diag}(w)x_0|^2 \sim (\frac{1}{n}\text{Exp}(1))^{\otimes n}$ if $w \sim \mathcal{CN}(0, I_n)$ and $\|x_0\| = 1$, thus

$$\mathbb{E}(\langle y_i, |F\text{Diag}(w_i^1)x_0|^2 - |F\text{Diag}(w_i^2)x_0|^2 \rangle) = \mathbb{E}(\langle \text{sign}(\theta(E_1) - \theta(E_2)), (E_1 - E_2) \rangle) = \lambda > 0.$$

Then the above assumption simply means that the one bit measurements preserve robustly the ranking of the intensities. Let \hat{x}_r be the maximum eigenvector of \hat{C}_r defined in (24). The following Theorem shows that \hat{x}_r is an ϵ -estimate of x_0 .

Theorem 1 (Phase Retrieval From One Bit Coded Diffraction Patterns). *For $x_0 \in \mathbb{C}^n, \|x_0\| = 1$, and $0 < \epsilon < 1$. Assume $y_1 \dots y_r$, follow the model given in (23). Then we have with a probability at least $1 - O(n^{-2})$,*

$$\text{for } r \geq \frac{c}{\epsilon^2 \lambda^2} \log^3 n, \quad \|\hat{x}_r - x_0 e^{i\phi}\|^2 \leq \epsilon$$

where c is a numeric constant, and $\phi \in [0, 2\pi]$ is a global phase. λ is given in (25).

For the noiseless model $\theta(z) = z$ and $\lambda = 1$. Thus the theorem states that $O(\log^3 n)$ pairs of coded diffraction patterns ensures the recovery of the phase. For different observation model θ it suffices to compute the value of λ as given in (25). We turn now to the noisy measurements setup (18) and show robustness of phase retrieval from one bit coded diffraction patterns:

Corollary 1 (One bit Recovery/ Noise). *For $x_0 \in \mathbb{C}^n, \|x_0\| = 1$, and $0 < \epsilon < 1$. Assume $y_1 \dots y_r$, follow the model given in (23), for $\theta(z) = z + \nu, \nu \sim \text{Exp}(\gamma)$. Where ν is an exponential noise with variance $\sigma = \frac{1}{\gamma^2}$. Then for any $\epsilon, 0 < \epsilon < 1$, we have with a probability at least $1 - O(n^{-2})$,*

$$\text{for } r \geq \frac{c}{\epsilon^2} \frac{(1 + \sqrt{\sigma})^4}{(1 + 2\sqrt{\sigma})^2} \log^3 n, \quad \|\hat{x}_r - x_0 e^{i\phi}\|^2 \leq \epsilon,$$

where c is a numeric constant, and $\phi \in [0, 2\pi]$ is a global phase.

In other words, under an exponential noise we have:

$$\|\hat{x}_r - x_0 e^{i\phi}\|_2^2 \leq C \sqrt{\frac{\log^3 n (1 + \sqrt{\sigma})^2}{r (1 + 2\sqrt{\sigma})}}.$$

Beyond robustness to noise, another desirable feature for phase retrieval from phase-less measurements, is the robustness to distortions of the values of intensities. Is it possible to retrieve the phase from coded diffraction patterns that are undergoing clipping for instance (as in equation (20))?

Corollary 2 (One bit Recovery/ Distortion). *For $x_0 \in \mathbb{C}^n, \|x_0\| = 1$, and $\epsilon > 0$. Assume $y_1 \dots y_m$, follow the model given in (23), for $\theta(z) = \tanh(\alpha z), \alpha > 0$. Then for any $\epsilon, 0 < \epsilon < 1$, we have with a probability at least $1 - O(n^{-2})$,*

$$\text{for } r \geq \frac{c \log^3 n}{\epsilon^2 \lambda^2(\alpha)}, \quad \|\hat{x}_r - x_0 e^{i\phi}\|^2 \leq \epsilon,$$

where c is a numeric constant, and $\phi \in [0, 2\pi]$ is a global phase. $\lambda(\alpha) = \mathbb{E}(|E_1 - E_2| \text{sign}(1 - \tanh(\alpha E_1) \tanh(\alpha E_2)))$, is a decreasing function in α .

For the last setup where the resolution of the observed diffraction patterns is limited by the Fraunhofer diffraction limit f_c of an optical system as in equation (21). We show that the recovery is still possible even if the PSF of the optical system was unknown. The number of modulations needed is poly-logarithmic in the dimension and quadratic in the super-resolution factor $SRF = \frac{n}{2f_c+1}$ defined in [FGC12].

Corollary 3 (One bit Recovery/Super-Resolution). *For $x_0 \in \mathbb{C}^n, \|x_0\| = 1$, and $0 < \epsilon < 1$. Assume $y_1 \dots y_m$, follow the model given in (23) for (b_i^1, b_i^2) defined as in (21) for a PSF h characterized by the cut-off frequency f_c . Then for $\epsilon, 0 < \epsilon < 1$, we have with we have with a probability at least $1 - O(n^{-2})$,*

$$\text{for } r \geq \frac{c}{\epsilon^2} (SRF)^2 \log^3 n, \quad \|\hat{x}_r - x_0 e^{i\phi}\|^2 \leq \epsilon.$$

where c is numeric constant, and $\phi \in [0, 2\pi]$ is a global phase. SRF is the super-Resolution factor defined as: $SRF = \frac{n}{2f_c+1}$.

It follows that:

$$r \geq \frac{c}{\epsilon^2} \log^3 n \quad \|\hat{x}_r - x_0 e^{i\phi}\|^2 \leq SRF\epsilon,$$

this dependency on the Super-Resolution Factor (SRF) is similar to results in [FGC12], where super-resolution is achieved via total variation norm minimization and linear measurements. Note that in [FGC12] the phase of the linear measurements, and the PSF h are assumed to be known. It is worth noting that in [FGC12] the super-resolution problem considered, is different from our setting as authors consider a harder problem: super-resolution from a single image, and a strong prior, namely a point sources model and a total variation norm minimization. In our case we have access to multiple coded diffraction patterns and this is known as multi-frame super-resolution see for example [Gus00] and references therein.

The proof of Corollary 3 is given in Section 4. Corollary 3 states a surprising fact: one bit coded diffraction patterns allow not only the super-resolution of the signal but also it leads to a blind deconvolution since the only information needed on h is its super-resolution factor SRF , its PSF might be completely unknown. Intuitively the random modulations push the high frequency content of x_0 to the frequency interval where the Fourier transform of h is non zero. The number of modulations needed is therefore naturally proportional to the SRF as shown in Corollary 3. Hence the high frequency content of x_0 is mapped to the lower end spectrum by modulation or masking. Phase retrieval from one bit coded diffraction patterns in a way estimates the missing phase, the missing high frequency content and corrects for the blur induced by the unknown PSF h .

Moreover this result is still true if the observation model was:

$$\begin{aligned} (b_i^1, b_i^2) &= (|FH_i \text{Diag}(w_i^1)x_0|^2, |FH_i \text{Diag}(w_i^2)x_0|^2) \quad i = 1 \dots r, \\ y_i &\in \{-1, 1\}^n, \quad y_i = \text{sign}(b_i^1 - b_i^2), \quad i = 1 \dots r, \end{aligned} \tag{26}$$

where H_i are Toeplitz matrices associated to different unknown stochastic perturbations h_i . We assume for simplicity that the Fourier transform of h_i are non zero in the same frequency domain (the result is still true if this was not the case we don't analyze this case in this paper). The only requirement is therefore to have the same perturbation on each considered pairs of coded diffraction patterns. For example in microscopy small perturbations will result in a change in the PSF. In astronomy in speckle imaging different h_i model different atmospheric perturbations in a long exposure acquisition.

Surprisingly one bit coded diffraction patterns allow blind deconvolution even in the case of varying PSFs.

2.1 Discussion and Perspectives

2.1.1 Discussion

We comment in this section on our results and compare them to the current state of the art and put them in the perspective of future research. Let f_j be a row of the DFT matrix.

For phase-lift, by inspecting the proof in [CLM13] we note that three factors govern the sample complexity $O(\log^4(n))$, the first two of them come from matrix concentration inequality and the last one is due to the golfing scheme:

- A bound on the measurements, $|f_j \text{Diag}(w)x_0|^2, j = 1 \dots m$: $|f_j \text{Diag}(w)x_0|^2 \leq \beta \log(n)$ with high probability.
- A bound on the the absolute values of the entries of the modulation $|w_i|^2, i = 1 \dots n$. In [CLM13], authors define a family of admissible modulation, such that among other conditions: $|w_i|^2 \leq M$, where M is a constant independent to the dimension. It is worth noting that this class of modulations as opposed to a complex Gaussian modulation, saves extra poly-logarithmic terms in the overall sample complexity of that approach.
- An extra $\log(n)$ in the sample complexity is needed for the golfing scheme.

In contrast in our case the saving of extra poly-logarithmic terms ($O(\log^3 n)$) comes from the nature of one bit coded diffraction patterns. Our one bit measurements are bounded by one, hence they do not contribute to the sample complexity. On the other hand our modulations are Complex Gaussian. Complex Gaussian modulations have their squared absolute values bounded with high probability $|w_i|^2 \leq \beta \log(n)$ and hence they contribute to the sample complexity.

2.1.2 Perspectives

Greedy Refinements. Indeed PhaseLift and one bit phase retrieval are not comparable since one achieves exact recovery and the other achieves approximate recovery. For an accuracy ϵ the sample complexity for one bit phase retrieval scales as $\frac{1}{\epsilon^2}$. As for the Gaussian case the Alternating minimization [NJS13] for coded diffraction patterns initialized with the one bit solution would guarantee a better dependency on ϵ , we leave that direction to a future research. We conjecture that $O(\log^3 n + \log \frac{1}{\epsilon} \log \log \frac{1}{\epsilon})$ pairs of coded diffraction patterns ensures ϵ recovery with the alternating minimization initialized with the one bit solution. Our experiments on both simulated data and images confirm that (See Section 6).

Non Gaussian Modulations or Masks. Another direction would be to investigate admissible modulation of [CLM13] and one bit measurements as they both enjoy dimensionless boundedness, we leave also that point to a future work.

Blind Deconvolution from Coded Diffraction Patterns. In microscopy the PSF of the lens is often known. One Bit solution is agnostic to the PSF, hence one bit phase retrieval offers a good initial point to the alternating minimization conditioned on the knowledge of the PSF: phase retrieval with blur correction (See Section 6). For an unknown PSF an open question remains on how to provably recover both the signal and the PSF, via alternating minimization suitably initialized.

2.2 Roadmap

The paper is organized as follows: In Section 3 we introduce the one bit coded diffraction patterns scheme and the corresponding phase recovery procedure. In section 4 we show how super-resolution can be tackled within our framework. We address algorithms and computational aspects in Sections 5 and 6. Finally we give the proofs in Section 8.

3 Quantizing Coded Diffraction Patterns

3.1 Preliminary Matrix Notation

Let $M \in \mathbb{C}^{n \times n}$ be a complex matrix, $diag(M)$ is a vector in \mathbb{C}^n , containing the diagonal elements of M .

Let $u \in \mathbb{C}^n$ be a complex vector, $Diag(u)$ is a matrix in $\mathbb{C}^{n \times n}$, with u on the diagonal and zeros elsewhere.

Let F be the discrete Fourier matrix, such that $F_{jk} = \frac{1}{\sqrt{n}} e^{-i \frac{2\pi(j-1)(k-1)}{n}}$, $j = 1 \dots n, k = 1 \dots n$.

3.2 One Bit Coded Diffraction Patterns

We start by defining the quantization scheme of the values of masked Fourier intensities or CDP. We assume that we observe $\theta(|FDiag(w^1)x_0|^2)$, where θ is eventually an unknown non linearity satisfying (25). Following the same procedure in the Gaussian case we quantize the differential of two independent coded diffraction patterns.

Definition 2 (One-bit Fourier quantizer). *Let $W = (w^1, w^2)$, where w^1, w^2 are i.i.d. complex Gaussian vectors $\mathcal{N}(0, \frac{1}{2}I_n) + i\mathcal{N}(0, \frac{1}{2}I_n)$. w^1 and w^2 are called Gaussian masks or modulations. Let F be the discrete Fourier matrix in $\mathbb{C}^{n \times n}$. For $x_0 \in \mathbb{C}^n$, a one bit quantizer of coded diffraction patterns is given by*

$$Q_W^\theta : \mathbb{C}^n \rightarrow \{-1, 1\}^n, \quad Q_A^\theta(x_0) = \text{sign}(\theta(|FDiag(w^1)x_0|^2) - \theta(|FDiag(w^2)x_0|^2)).$$

where $|FDiag(w^1)x_0|^2$ is the complex modulus of each component of $FDiag(w^1)x_0$. θ is the observation model. θ is eventually an unknown non linearity that satisfies equation (25).

Recall that a basic quantizer in the noiseless case is obtained setting $\theta(z) = z$.

Now for a total of $2r$ masks or modulations we define the one bit coded diffraction patterns:

Definition 3 (One Bit Coded Diffraction Patterns). *Let $\{W_i = (w_i^1, w_i^2)\}_{1 \leq i \leq r}$, be $2r$ i.i.d. Gaussian masks in \mathbb{C}^n , and $Q_{W_i}^\theta(x_0)$ as in Def 2. The Quantized Phase-less sensing is : $\mathcal{Q} : \mathbb{C}^n \rightarrow \{-1, 1\}^{nr}$, $\mathcal{Q}(x_0) = (Q_{W_1}^\theta(x_0), \dots, Q_{W_m}^\theta(x_0))$.*

Let

$$y_i = \text{sign}(\theta(|FDiag(w_i^1)x|^2) - \theta(|FDiag(w_i^2)x|^2)) \in \{-1, 1\}^n \quad i = 1 \dots r \quad (27)$$

In this paper, we are interested in recovering x_0 from its one bit coded diffraction patterns $y = (y_1 \dots y_m) = \mathcal{Q}(x_0)$. It is easy to see that the phase retrieval amounts to the following feasibility problem:

$$\begin{aligned} & \text{find } x \\ & \text{subject to} \\ & \langle y_i, |FDiag(w_i^1)x|^2 - |FDiag(w_i^2)x|^2 \rangle \geq 0, \quad i = 1 \dots r. \\ & \|x\|^2 = 1. \end{aligned} \quad (28)$$

Again we propose the following relaxation to tackle that problem:

$$\max_{x, \|x\|_2=1} \left(\frac{1}{r} \sum_{i=1}^r \langle y_i, |FDiag(w_i^1)x|^2 - |FDiag(w_i^2)x|^2 \rangle \right) \quad (29)$$

The proof architecture is similar to the Gaussian case. Proofs are given in Section 8. We start by a preliminary definition:

Definition 4 (Fourier Risk and Empirical risk). *Let $x_0 \in \mathbb{C}^n, \|x_0\| = 1$. For $x \in \mathbb{C}^n$ such that $\|x\| = 1$, and $W = \{w^1, w^2\}$ i.i.d. complex Gaussians, let*

$$\mathcal{E}^{x_0}(x) = \mathbb{E}(\langle y, |FDiag(w^1)x|^2 - |FDiag(w^2)x|^2 \rangle),$$

where $y = \text{sign}(|FDiag(w^1)x_0|^2 - |FDiag(w^2)x_0|^2) \in \{-1, 1\}^n$. Moreover, let

$$\hat{\mathcal{E}}^{x_0}(x) = \frac{1}{r} \sum_{i=1}^r \langle y_i, |FDiag(w_i^1)x|^2 - |FDiag(w_i^2)x|^2 \rangle,$$

$y_i = Q_{W_i}^\theta(x_0)$ and $W_i = \{(w_i^1, w_i^2)\}, i = 1 \dots r$ are i.i.d. complex Gaussians.

In the following definition the phase retrieval problem is cast as an empirical risk maximization:

Definition 5 (Phase retrieval Problem). *The phase retrieval problem amounts to solving:*

$$\max_{x, \|x\|=1} \hat{\mathcal{E}}^{x_0}(x)$$

Let $\hat{x}_r = \arg \max_{x, \|x\|=1} \hat{\mathcal{E}}^{x_0}(x)$.

The following proposition shows that the objective function can be written explicitly as a quadratic form.

Proposition 1. $\mathcal{E}^{x_0}(x)$ can be rewritten as the following quadratic form:

$$\mathcal{E}^{x_0}(x) = x^* C x, \quad (30)$$

where $C = \mathbb{E}(\text{Diag}(w^1)FDiag(y)F^*\text{Diag}(w^{1,*}) - \text{Diag}(w^2)FDiag(y)F^*\text{Diag}(w^{2,*}))$. and

$$\hat{\mathcal{E}}^{x_0}(x) = x^* \hat{C}_r x, \quad (31)$$

where $\hat{C}_r = \frac{1}{r} \sum_{i=1}^r (\text{Diag}(w_i^1)FDiag(y_i)F^*\text{Diag}(w_i^{1,*}) - \text{Diag}(w_i^2)FDiag(y_i)F^*\text{Diag}(w_i^{2,*}))$.

The phase retrieval problem from One bit CDP is therefore a maximum eigenvalue problem, that we call *1bitPhase*:

$$\max_{x, \|x\|=1} x^* \hat{C}_r x \quad (32)$$

3.3 Theoretical analysis: Correctness in Expectation and Concentration

In this section we sketch the main steps of the proof of Theorem 1. The reader is referred to Section 8 for detailed proofs.

The following proposition shows that x_0 is indeed the leading eigen-vector of the expected problem (30) with eigen-value λ , where λ is given in (25). Moreover the expected matrix C is rank one:

Proposition 2 (Correctness in Expectation). *The following statements hold:*

1. For all $x \in \mathbb{C}^n$, $\|x\| = 1$, we have the following equality,

$$\mathcal{E}^{x_0}(x) = x^* C x = \lambda |\langle x_0, x \rangle|^2. \quad (33)$$

2. Let $y = Q_A^\theta(x_0)$, C is a rank one matrix,

$$C = \lambda x_0 x_0^*. \quad (34)$$

3. x_0 is an eigenvector of C with eigenvalue λ ,

$$C x_0 = \lambda x_0. \quad (35)$$

4. The maximum eigenvector of C is of the form $x_0 e^{i\phi}$, where $\phi \in [0, 2\pi]$. The maximum eigenvalue is given by λ .

The following lemma is a comparison equality that allows us to bound $\|x x^* - x_0 x_0^*\|_F^2$, for any point x , by the excess risk $\mathcal{E}^{x_0}(x_0) - \mathcal{E}^{x_0}(x)$:

Lemma 1. *The following equality holds for all $x \in \mathbb{C}^n$:*

$$\mathcal{E}^{x_0}(x_0) - \mathcal{E}^{x_0}(x) = \frac{\lambda}{2} \|x x^* - x_0 x_0^*\|_F^2.$$

The rest of the proof follows from empirical processes theory [LT91] and concentration inequalities [Tro12].

Proposition 3 (Concentration). *Let*

$$\hat{x}_r = \arg \max_{x, \|x\|=1} x^* \hat{C}_r x,$$

The following inequalities hold:

- 1.

$$\frac{\lambda}{2} \|\hat{x}_r \hat{x}_r^* - x_0 x_0^*\|_F^2 \leq 2 \|\hat{C}_r - C\|.$$

- 2.

$$\text{For } 0 < \epsilon < 1, r \geq c \frac{\log^3 n}{\epsilon^2}, \quad \|\hat{C}_r - C\| \leq \epsilon \text{ with probability at least } 1 - O(n^{-2}).$$

Proof of Theorem 1. The proof of Theorem 1 follows from a simple combination of Proposition 2, Lemma 1 and Proposition 3. \square

Proofs of Corollaries 1 and 2 are simple consequences of Theorem 1 and Lemma 2, where we specify the value of λ for each model.

Lemma 2. *The values of λ for different observation models θ are given in the following:*

1. *Noiseless setup: $\theta(z) = z$, $\lambda = 1$.*
2. *Noisy setup: $\theta(z) = z + \nu$, ν is an exponential random variable with variance σ , $\lambda = \frac{1+2\sqrt{\sigma}}{(1+\sqrt{\sigma})^2}$.*
3. *Distortion setup: $\theta(z) = \tanh(\alpha z)$, where $\alpha > 0$, $\lambda = \mathbb{E}(\text{sign}(1 - \tanh(\alpha E_1) \tanh(\alpha E_2)) |E_1 - E_2|)$ is a decreasing function in α .*

4 From One bit Coded Diffraction Patterns to Super-Resolution

We turn now to the problem of recovering a signal from its lower end of power spectra. As discussed earlier this is a problem of practical interest, as the resolution of an optical system, for instance a lens h is limited by the Fraunhofer diffraction limit f_c . The super-resolution factor of h is therefore defined as $SRF = \frac{n}{2f_c+1}$. In our setup the modulated signal diffracts through a lens characterized by a PSF h and a cut-off frequency f_c . Hence instead of observing the power spectra of the modulated signal $Diag(w)x_0$ we observe the power spectra of a lower resolution signal namely $h \star (Diag(w)x_0)$. Let \hat{u} be the Fourier transform of $u \in \mathbb{C}^n$, $\hat{u} = Fu$. Note that by the properties of the Fourier transform we have:

$$F(h \star (Diag(w)x_0)) = \hat{h} \odot \widehat{Diag(w)x_0} \quad (36)$$

Hence we observe :

$$|F(h \star (Diag(w)x_0))|^2 = |\hat{h}|^2 \odot |\widehat{Diag(w)x_0}|^2 \quad (37)$$

In this section we re-index k for convenience $-\frac{n}{2} \leq k \leq \frac{n}{2} - 1$. We use also the following convention $\text{sign}(0) = 1$, this choice is arbitrary. Note that due to the diffraction limit f_c , h satisfies:

$$|\hat{h}|_k^2 = 0, \text{ for } k \notin \llbracket -f_c, f_c \rrbracket.$$

Hence our phase-less measurement are missing in high frequencies ranges:

$$b_k = |\hat{h}|_k^2 |\widehat{Diag(w)x_0}|_k^2 \quad k \in \llbracket -f_c, f_c \rrbracket \text{ and } b_k = 0 \text{ elsewhere.} \quad (38)$$

The one bit coded diffraction patterns are the defined by comparing pairs of low resolution coded diffraction patterns (b^1, b^2) defined as in (38) for two independent modulations $w^1, w^2 \sim \mathcal{CN}(0, I_n)$.

$$y_k = \text{sign}(b_k^1 - b_k^2), k = 1 \dots n,$$

Note that $y_k = 0$ if $k \notin \llbracket -f_c, f_c \rrbracket$. For all $k \in \llbracket -f_c, f_c \rrbracket$, we have $(d_k^1 = |FDiag(w^1)x_0|_k^2, d_k^2 = |FDiag(w^2)x_0|_k^2) \sim (\frac{1}{n}E_k^1, \frac{1}{n}E_k^2)$, where E_k^1, E_k^2 iid $Exp(1)$. We are now ready to compute the value of λ corresponding to that observation model:

$$\begin{aligned} \lambda &= \mathbb{E}(\langle y, |FDiag(w^1)x_0|^2 - |FDiag(w^2)x_0|^2 \rangle) \\ &= \sum_{k=-\frac{n}{2}}^{\frac{n}{2}-1} \mathbb{E}(\text{sign}(b_k^1 - b_k^2)(d_k^1 - d_k^2)). \end{aligned}$$

Note that:

$$\text{For } k \in \llbracket -f_c, f_c \rrbracket \quad \text{sign}(b_k^1 - b_k^2) = \text{sign}\left(|\hat{h}_k|^2 d_k^1 - |\hat{h}_k|^2 d_k^2\right) = \text{sign}\left(|\hat{h}_k|^2 (d_k^1 - d_k^2)\right) = \text{sign}(d_k^1 - d_k^2). \quad (39)$$

it follows that:

$$\begin{aligned} \lambda &= \sum_{k \in \llbracket -f_c, f_c \rrbracket} \mathbb{E}\left(\text{sign}(d_k^1 - d_k^2)(d_k^1 - d_k^2)\right) \\ &= \frac{1}{n} \sum_{k \in \llbracket -f_c, f_c \rrbracket} \mathbb{E}\left(\text{sign}(E_k^1 - E_k^2)(E_k^1 - E_k^2)\right) \\ &= \frac{2f_c + 1}{n} \mathbb{E}(|E^1 - E^2|) \\ &= \frac{2f_c + 1}{n}. \\ &= \frac{1}{SRF}. \end{aligned}$$

Thus we find that λ is the inverse of the super-resolution factor, which confirms our findings on λ as a quality factor: λ is small when the cut off frequency is small. Interestingly λ depends only on the domain of \hat{h} , regardless the shape or the values of the corresponding PSF , and this is due to the quantization step in (39). This the main reason behind the feasibility of blind deconvolution within our framework. Corollary 3 follows simply from Theorem 1 setting $\lambda = \frac{1}{SRF}$.

5 Algorithms and Computations

5.1 One Bit Phase Retrieval Algorithm

A straight forward computation of the maximum eigenvector of \hat{C}_r is rather expensive. Using the power method, and the Fast Fourier transform we get a computational complexity of

$$O(n \log^4(n)).$$

Note by FFT the Fast Fourier Transform and iFFT the Inverse Fast Fourier Transform. For the power method we need to compute $\hat{C}_r u$:

$$\begin{aligned} \hat{C}_r u &= \frac{1}{r} \sum_{i=1}^r \text{Diag}(w_i^1) F \text{Diag}(y_i) F^* \text{Diag}(w_i^{1,*}) u - \text{Diag}(w_i^2) F \text{Diag}(y_i) F^* \text{Diag}(w_i^{2,*}) u \\ &= \frac{1}{r} \sum_{i=1}^r w_i^1 \odot \text{FFT}\left(y_i \odot i\text{FFT}(w_i^{1,*} \odot u)\right) - w_i^2 \odot \text{FFT}\left(y_i \odot i\text{FFT}(w_i^{2,*} \odot u)\right) \end{aligned}$$

For each iteration we need to compute the FFT for each pairs of modulations, that costs $O(n \log(n))$ per pair. We have $O(\log^3 n)$ pairs, hence a total of $O(n \log^4(n))$ operations per iteration of the power method.

Algorithm 1 FastFourier1bitCDPPHasePower

```
1: procedure FASTFOURIER1BITCDPPHASEPOWER( $\{w_i^1, w_i^2\}_{i=1\dots r}, y = (y_1 \dots y_r), \epsilon$ )
2:   Initialize  $r_0$  at random,  $j = 1$ .
3:   while  $\|u_j - u_{j-1}\| > \epsilon$  or  $j = 1$  do
4:      $u_j^1 \leftarrow \frac{1}{r} \sum_{i=1}^r w_i^1 \odot \text{FFT} \left( y_i \odot \text{iFFT} \left( w_i^{1,*} \odot u_{j-1} \right) \right)$ 
5:      $u_j^2 \leftarrow \frac{1}{r} \sum_{i=1}^r w_i^2 \odot \text{FFT} \left( y_i \odot \text{iFFT} \left( w_i^{2,*} \odot u_{j-1} \right) \right)$ 
6:      $u_j \leftarrow u_j^1 - u_j^2$ 
7:      $\hat{\lambda} \leftarrow \|u_j\|$ 
8:      $r_j \leftarrow \frac{u_j}{\hat{\lambda}}$ 
9:      $j \leftarrow j + 1$ 
10:  end while
11:  return  $(\hat{\lambda}, u)$   $\triangleright (\hat{\lambda}, u)$  is an estimate of  $(\lambda, x_0)$ .
12: end procedure
```

5.2 SubExp Initialization

In this spirit of the initialization *SubExpPhase* proposed in [NJS13] for Gaussian measurements we propose the following initialization from coded diffraction patterns. Let $b_i = |F \text{Diag}(w_i) x_0|^2$, $i = 1 \dots L$, where $w_i \sim \mathcal{CN}(0, I_n)$ iid. Define

$$\hat{C}_L = \frac{1}{L} \sum_{i=1}^L \text{Diag}(w_i) F \text{Diag}(b_i) F^* \text{Diag}(w_i^*),$$

It is possible to show that:

$$\mathbb{E}(\hat{C}_L) = x_0 x_0^* + I_n,$$

we omit the proof and refer the reader to Lemma 3.1 in [CLM13] for a similar argument. As in the case of the Gaussian measurements the sample complexity of *SubExpPhase* is higher than One bit Phase Retrieval. An inspection of the proof of one bit phase retrieval shows that $O(\log^5 n / \epsilon^2)$ modulations are needed for an ϵ recovery in *SubExpPhase* (we omit the details and show that this is indeed encountered in practice in Section 6.1.1). Let \hat{x}_L be the maximum eigenvector of \hat{C}_L , \hat{x}_L is a good proxy of x_0 , hence the following algorithm that proceeds by the power method in order to find the maximum eigenvector:

Algorithm 2 FastFourierSubExpCDPPHasePower

```
1: procedure FASTFOURIERSUBEXPCDPPHASEPOWER( $\{w_i^1, w_i^2\}_{i=1}^r, b = ((b_i^1, b_i^2) \dots (b_r^1, b_r^2)), \epsilon$ )
2:   Initialize  $r_0$  at random,  $j = 1$ .
3:   while  $\|u_j - u_{j-1}\| > \epsilon$  or  $j = 1$  do
4:      $u_j \leftarrow \frac{1}{r} \sum_{i=1}^r w_i^1 \odot \text{FFT} \left( b_i^1 \odot \text{iFFT} \left( w_i^{1,*} \odot u_{j-1} \right) \right) + w_i^2 \odot$   

        $\text{FFT} \left( b_i^2 \odot \text{iFFT} \left( w_i^{2,*} \odot u_{j-1} \right) \right)$ 
5:      $\hat{\lambda} \leftarrow \|u_j\|$ 
6:      $r_j \leftarrow \frac{u_j}{\hat{\lambda}}$ 
7:      $j \leftarrow j + 1$ 
8:   end while
9:   return  $(\hat{\lambda}, u)$   $\triangleright (\hat{\lambda}, u)$  is an estimate of  $(\lambda, x_0)$ .
10: end procedure
```

5.3 Alternating Minimization Initialized with the One Bit Solution or the solution *SubExpPhase*

Given the one bit solution or the solution of *SubExpPhase* we can refine the solution, by running the alternating minimization procedure on the actual coded diffraction patterns initialized with the one bit solution or with the solution of *SubExpPhase* as follows:

Algorithm 3 FastAltMin+OneBitCDP initialization

```

1: procedure ALTMINPHASE( $w_1^1, w_2^2, \dots, w_r^1, w_r^2, b = (\sqrt{b_1^1}, \sqrt{b_1^2} \dots \sqrt{b_r^1}, \sqrt{b_r^2}), \epsilon$ )
2:   Initialize  $x \leftarrow \text{FASTFOURIER1BITCDPPHASEPOWER}(\{w_i^1, w_i^2\}_{i=1 \dots r}, y = (y_1 \dots y_r), \epsilon)$  or
    $x \leftarrow \text{FASTFOURIERSUBEXPCDPPHASEPOWER}\{w_i^1, w_i^2\}_{i=1 \dots r}, b = (b_1 \dots b_{2r}), \epsilon$ 
3:   for  $k = 1 \dots t_0$  do ▷  $t_0$  is the number of iterations.
4:      $(u_1^1, u_1^2, \dots, u_r^1, u_r^2) \leftarrow (\text{Ph}(\text{FFT}(w_1^1 \odot x)), \text{Ph}(\text{FFT}(w_1^2 \odot x)), \dots)$ 
5:      $x \leftarrow \frac{1}{\sum_{s=1}^r (|w_s^1|^2 + |w_s^2|^2)} \odot \left( \sum_{i=1}^r w_i^{1*} \odot i\text{FFT}(\sqrt{b_i^1} \odot u_i^1) + w_i^{2*} \odot i\text{FFT}(\sqrt{b_i^2} \odot u_i^2) \right)$ 
6:   end for
7:   return  $x$ 
8: end procedure

```

The computational complexity of Algorithm 3 is $O(n \log^4 n)$ by iteration. The full analysis of this algorithm is subject to future research.

6 Numerical Experiments

6.1 One Dimensional Simulations

In this section we test our algorithms on one dimensional simulated signals. We consider $x_0 \in \mathbb{R}^n$, such that x_0 is a gaussian vector, $x_0 \sim \mathcal{N}(0, I_n)$, we set $n = 8000$. We first study the phase transition of One Bit Phase Retrieval and compare it to its counterpart in *SubExpPhase* in Section 6.1.1. We then show in Section 6.1.2 the robustness of One Bit phase retrieval, to noise, distortion and blur .

6.1.1 Phase Transition of One Bit Phase Retrieval Versus *SubExpPhase*

We consider in this section how the performance of Algorithm 1 for *1bitPhase* and Algorithm 2 for *SubExpPhase* depend on the number of measurements. We consider 50 trials , where we generate pairs of CDP $(b_\ell^1, b_\ell^2), \ell = 1 \dots r$ according to Equation (22) and the one bit CDP $y_\ell, \ell = 1 \dots r$, according to (23), where we set θ to be the identity (noiseless model).

At each trial we generate a set of new random modulation, and run Algorithms 1 (*1bitPhase*) and 2 (*SubExpPhase*).

In Figure 1, we report the empirical probability of success of each algorithm for increasing number of measurements r . We have a success if the error $1 - |\langle \hat{x}_r, x_0 \rangle|^2 < \tau$. We set $n = 8000, \tau = 0.07$ in this experiment. We see that the phase transition for *1bitPhase* happens earlier than the one for *SubExpPhase*, which confirms that One Bit Phase retrieval allows lower sample complexity for a given precision.

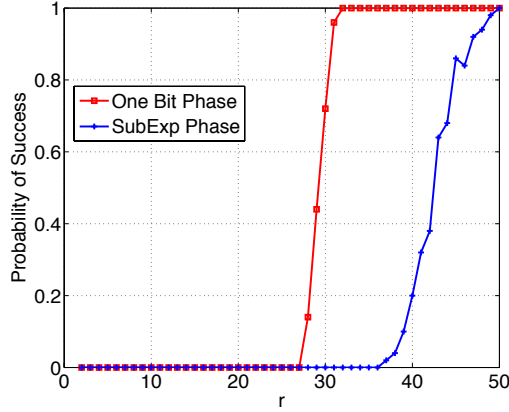
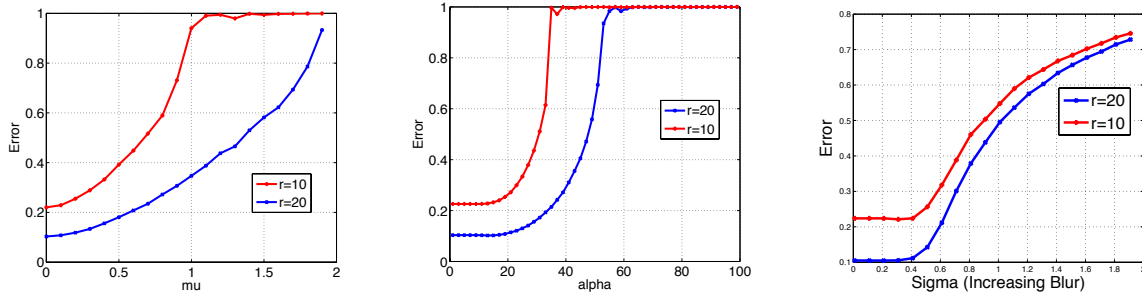


Figure 1: Phase transition comparison of one bit Phase retrieval and SubExp phase Retrieval.

6.1.2 Robustness

We test the robustness of Algorithm 1 to noise, distortion, and blur. For this end we generate measurements according to the noise model given in Equation (18), for increasing noise level and for $r = 10$ and $r = 20$. We see in Figure 2(a) that that the recovery error of One Bit Phase Retrieval increases gracefully with the level of noise and as more measurements are available the error of recovery drops down. In the setup of distorted measurements we generate CDP according to Equation (21), for different distortion levels α , for different number of measurements $r = 10$, and $r = 20$. We see in Figure 2(b) that the recovery is still possible thanks to the robustness of One Bit Phase Retrieval, despite the severe non linearity. Finally we test the robustness of *1bitPhase* to a gaussian blur with increase aperture. We generate our CDP according to the blurry model in Equation (21), for $r = 10$ and $r = 20$. We see in Figure 2(c) that phase retrieval and Super-Resolution are possible with One Bit Phase Retrieval and that the error increases gracefully also with the size of the aperture and drops as more measurements are available.



(a) Robustness to Exponential noise: Error $1 - |\langle x, x_0 \rangle|^2$ versus μ the mean of the Exponential noise
(b) Robustness to distortion: Error $1 - |\langle x, x_0 \rangle|^2$ versus α the size of the clipping.
(c) Robustness to blur: Error $1 - |\langle x, x_0 \rangle|^2$ versus σ the aperture of a gaussian filter.

Figure 2: Phase transition comparison of one bit Phase retrieval and SubExp phase Retrieval.

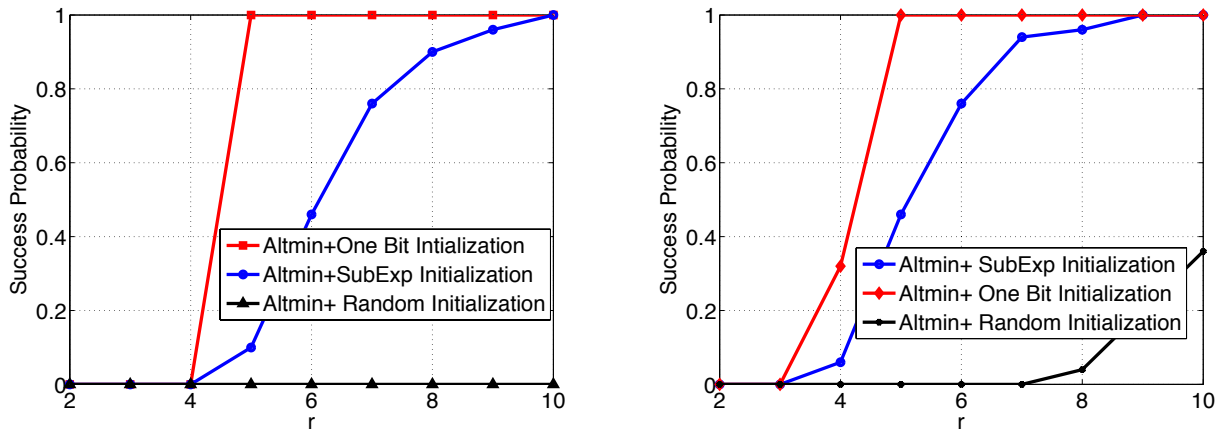
6.1.3 One Bit Phase Retrieval and Alternating Minimization

Alternating Minimization Phase Transition. As discussed in Section 2.1.2, and Section 5.3, greedy refinements of the solution of *1bitPhase* and *SubExpPhase*, enhance the quality of the recovery and the sample complexity of the overall procedure as showed in [NJS13] for the Gaussian measurements. Extending those results to Coded Diffraction patterns is subject to future work. We conjecture on one hand that AM initialized with the one bit solution has a sample complexity of $O(\log^3 n + \log \frac{1}{\epsilon} \log \log \frac{1}{\epsilon})$, and on the other hand that AM initialized with *SubExpPhase* solution has a sample complexity of $O(\log^5 n + \log \frac{1}{\epsilon} \log \log \frac{1}{\epsilon})$. We show in the next section the phase transition of AM (Algorithm 3) initialized with *1bitPhase*, *SubExpPhase* and a random initialization in the noisy and the noiseless case.

In order to highlight the effect of the initialization step in the AM Algorithm 3, we fix the number of iterations to $t_0 = 50$ in the noiseless and the noisy setting.

In figure 3(a) we report the empirical success probability of Algorithm 3 in the noiseless setting versus the number of pairs of modulations r . We declare in the noiseless case a success if $\|\hat{x}_{t_0} \hat{x}_{t_0}^* - x_0 x_0^*\|_F < 10^{-5}$. We see that with that relatively small number of iterations, the phase transition of AM initialized with One Bit Phase solution happens at $r = 4$. AM initialized with *SubExpPhase* with that limited number of iterations needs more samples to achieve phase transition at $r = 10$. AM initialized at random does not achieve its phase transition with that limited number of samples and iterations. This phase transition confirms the lower sample complexity of one bit solution, and its greedy refinements.

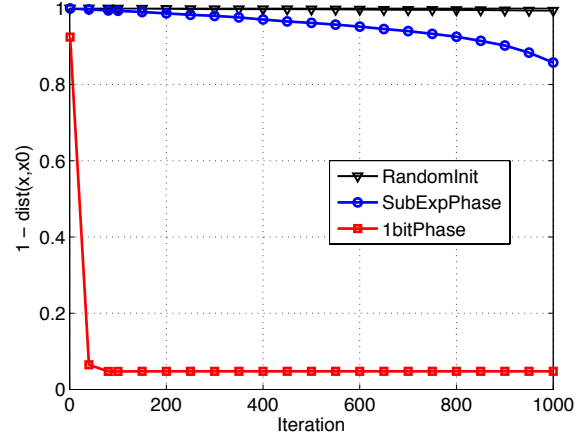
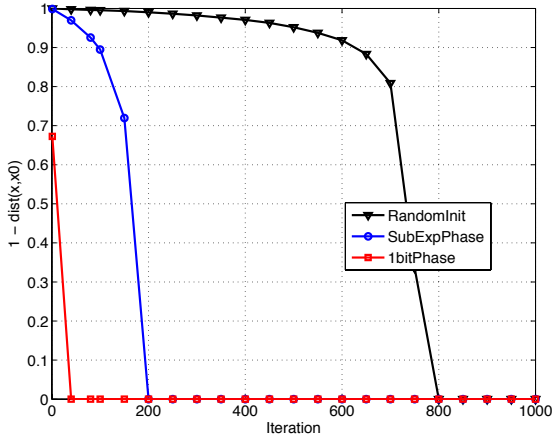
We now turn to the noisy setting (18) where we set $\sigma = 0.04$. In figure 3(b) we report the empirical success probability of Algorithm 3, where we declare in this setting a success if $\|\hat{x}_{t_0} \hat{x}_{t_0}^* - x_0 x_0^*\|_F < 0.03$. We see that at that accuracy level, the greedy refinements of one bit solutions are still robust to noise and superior to the other forth-mentioned initializations (*SubExpPhase* and random).



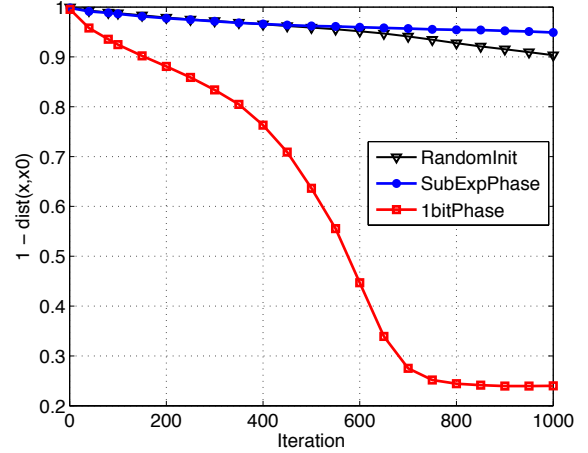
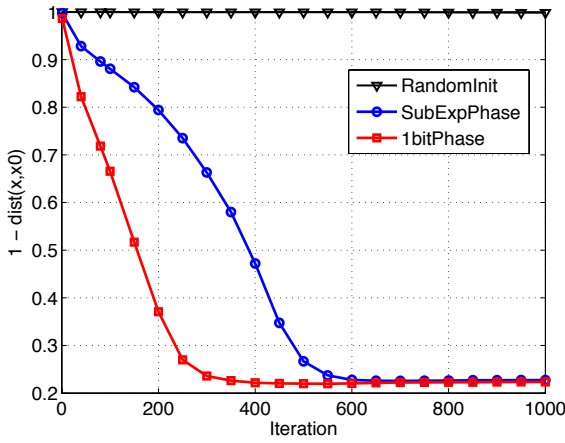
(a) Alternating Minimization's phase transition in the noiseless setting. (b) Alternating Minimization's phase transition in the noisy setting.

Figure 3: Phase transition comparison of one bit Phase retrieval and SubExp phase Retrieval.

Error Decay. To illustrate the benefit of the initialization step in AM we report in the following the error decay of AM with different initializations. In figure 4(a) we see that in the noiseless setting all approaches converge, the convergence is faster for AM initialized with the one bit solution in high dimension. In figure 4(b), 4(c), 4(d) we see that AM initialized with one bit solution is more robust in the noisy setting.



(a) Error $1 - |\langle x, x_0 \rangle|^2$ versus Iterations of AltMinPhase, (b) Error $1 - |\langle x, x_0 \rangle|^2$ versus Iterations of AltMinPhase, for $n = 8000$, and a total measurements $8n$ in the noiseless $n = 8000$ and a total measurements $8n$ in the noisy setting $\sigma = 0.4$.



(c) Error $1 - |\langle x, x_0 \rangle|^2$ versus Iterations of AltMinPhase, for $n = 8000$ and a total measurements $8n$ in the noisy setting $n = 8000$ and a total measurements $8n$ in the noisy setting $\sigma = 0.8$. (d) Error $1 - |\langle x, x_0 \rangle|^2$ versus Iterations of AltMinPhase, for $n = 8000$ and a total measurements $8n$ in the noisy setting $n = 8000$ and a total measurements $8n$ in the noisy setting $\sigma = 0.8$.

Figure 4: Alternating minimization convergence with different initializations: Random Initialization, 1bitPhase, and SubExpPhase, in the noisy and noiseless setting.

In the next section we test our algorithms in imaging applications, which highlights the efficiency and the robustness of the algorithms in potential applications in microscopy, astronomy and X-ray Crystallography.

6.2 Imaging Applications

We address in this section the problem of phase recovery in imaging applications. In the following we consider two test images, and their respective power spectra. The image in Figure 5 has a dominant edge structure, and the image in Figure 6 has a dominant textured content. We show that the same algorithms presented in this paper allow the phase recovery, where we simply replace the vectors with $2D$ arrays and the $1D$ FFT with the $2D$ FFT.

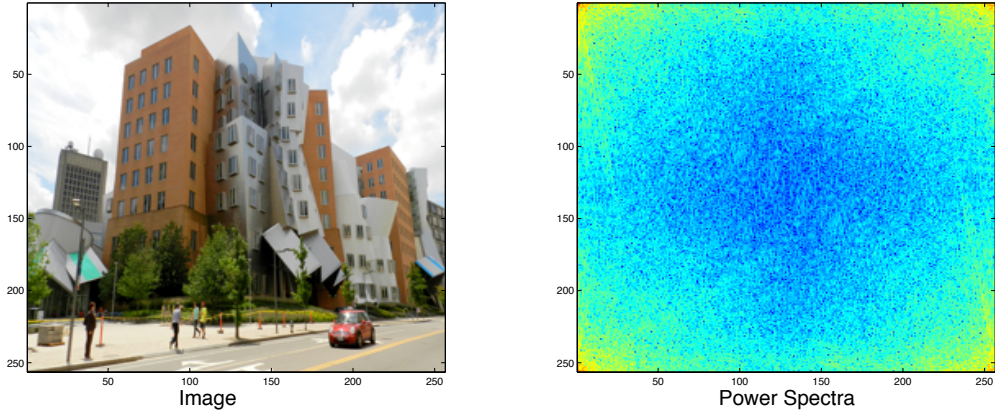


Figure 5: An image of Stata Center (Structured) and its Power Spectra (we plot the logarithm of the power spectra of one color Channel (R for instance)).

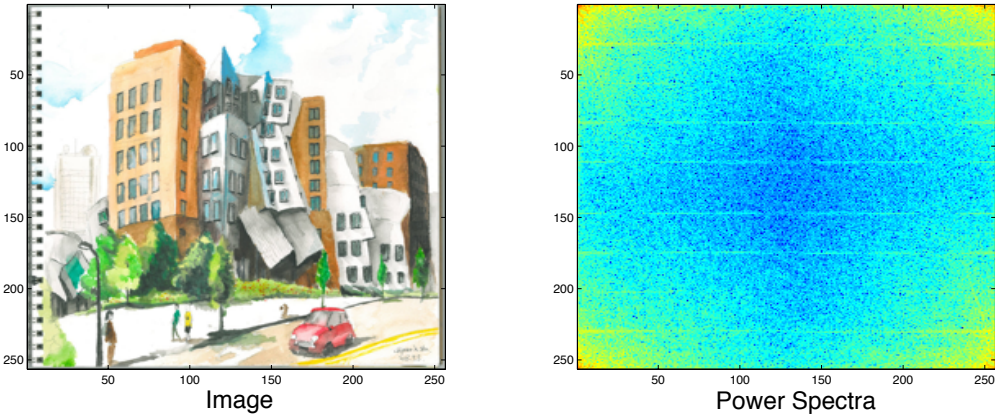


Figure 6: A drawing of Stata Center (texture like image) and its Power Spectra (we plot the logarithm of the power spectra of one color Channel (R for instance)).

6.2.1 One Bit Coded Diffraction Patterns

We modulate the image with a $2D$ Gaussian array and collect $2D$ coded diffraction patterns. We illustrate in Figure 7 the one bit coded diffraction patterns that become in this case a $2D$ binary array. The one bit array is obtained by quantizing pairs of coded diffraction arrays. Our goal is therefore to recover robustly the image from the knowledge of One bit coded diffraction arrays using the same algorithms presented in this paper. In the next section we test the robustness of the recovery against distortion, noise and blur.

6.2.2 Phase Retrieval from Distorted Diffraction Patterns.

In many acquisition systems we collect the power spectra of an object of interest. This acquisition might be altered by many imperfections due to multiple scattering phenomena for instance, or distortion in the precision of the CCD. Robustness to distortion such as clipping is a desirable feature in phase retrieval. In Figure 8 we simulate distorted power spectra by applying a sigmoid

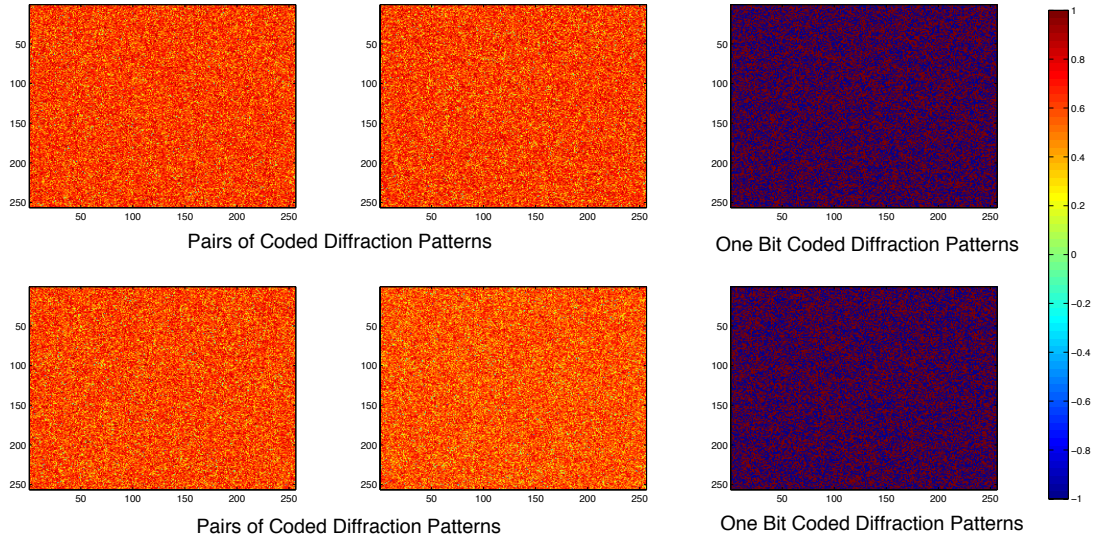


Figure 7: One Bit Coded Diffraction Patterns obtained by quantizing pairs of coded diffractions patterns.

($\tanh(\alpha \cdot)$) to the Fourier spectrum, for different clipping levels (α). While most of the spatial frequency information is lost, phase retrieval is still possible thanks to the robustness of One Bit Phase retrieval to distortions. We apply $2r$ Gaussian masks to our image of interest and then collect the power spectra of each masked image. We apply to each masked power spectra a sigmoid with a clipping parameter α . We then get our One Bit CDP by quantizing pairs of distorted power spectra. In our experiment $n = 256 \times 256$, $r = 16 \lfloor \log(n) \rfloor$.

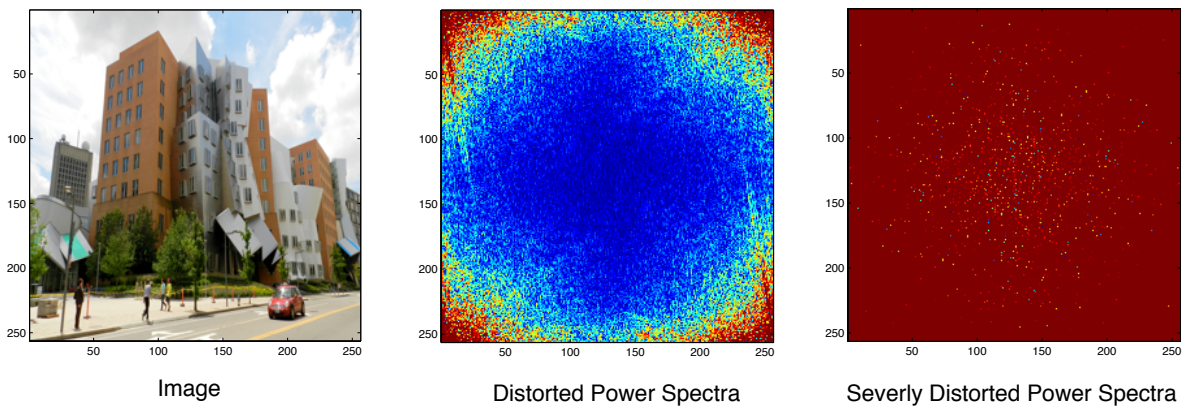


Figure 8: Stata Center's power spectra undergoing a distortion such as clipping of the values $\tanh(\alpha |\hat{x}(w)|)$. The distorted power spectra is obtained for $\alpha = 0.001$. The severely distorted is obtained for $\alpha = 0.1$.

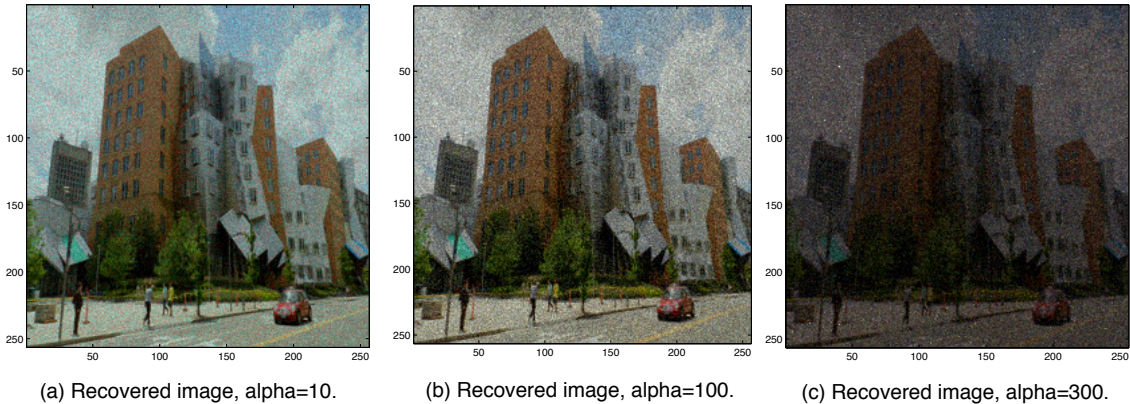


Figure 9: One Bit Phase Retrieval from distorted CDP. (a) and (b) Recovery from small distortions. (c) Recovery from Severe Distortions.

We run independently the same process of acquisition on the three color channels, as well as Algorithm 1. In Figures 9 and 10 we show the output of the Algorithm 1 for various level of distortions varying from mild to severe distortion. We see that the reconstruction in both cases is still possible from one bit CDP despite the distortion that the intensities values are undergoing.

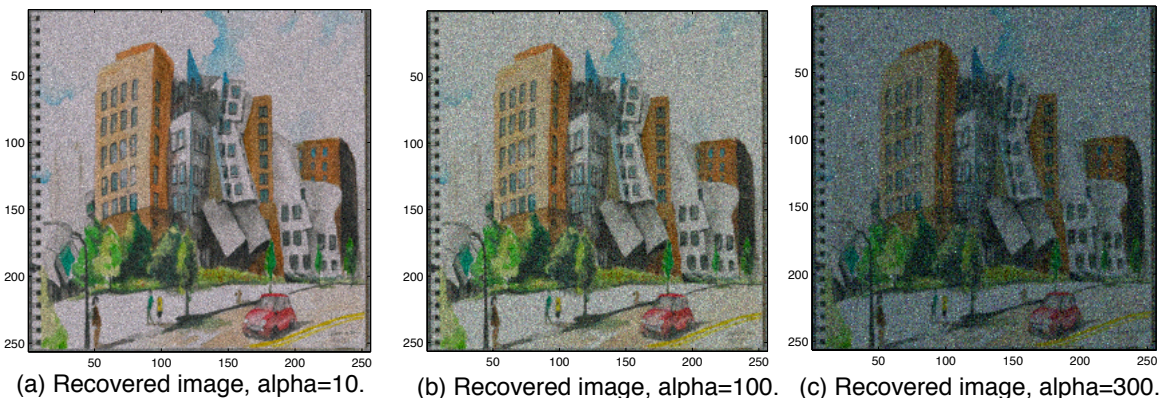


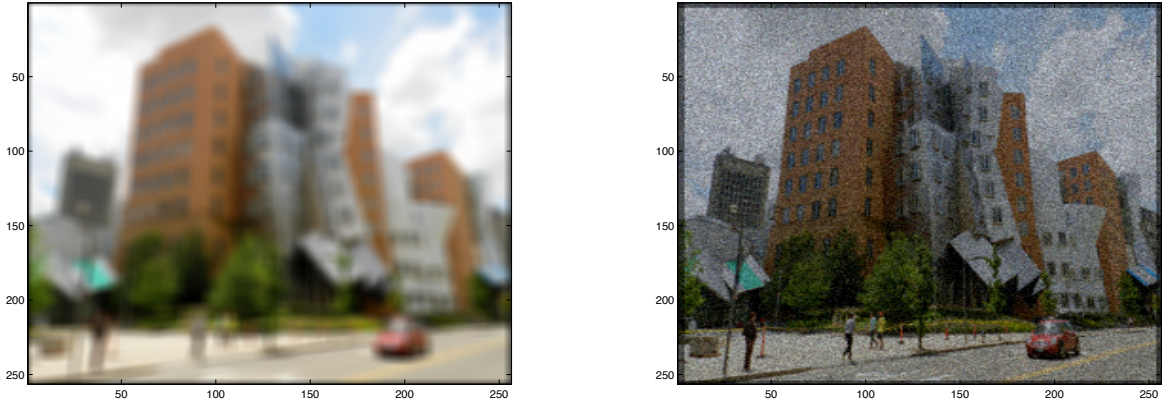
Figure 10: One Bit Phase Retrieval from distorted CDP. (a) and (b) Recovery from small distortions. (c) Recovery from Severe Distortions.

6.2.3 Super-Resolution and Blind Deconvolution

We turn now to the problem of recovering an image from its lower end of power spectra. As discussed earlier this is a problem of practical interest in microscopy, as the resolution of an optical system, for instance a lens h is limited by the Fraunhofer diffraction limit f_c . The super-resolution factor of h is therefore defined as $SRF = \frac{n}{2f_c + 1}$. In our setup the modulated object diffracts through a lens characterized by a PSF h and a cut-off frequency f_c . Hence instead of observing the power spectra of the modulated signal $Diag(w)x_0$ we observe the power spectra of a lower resolution signal namely $h \star (Diag(w)x_0)$. We consider in this experiment h to be an averaging filter. In Figure 11(a) we see a blurred image, obtained by convolving the original image Stata with an averaging filter of size 8×8 . In the following we simulate the diffraction patterns of the modulated image

through the aperture h by taking: $(|Fh \star (\text{Diag}(w_i^1)x_0)|^2, |Fh \star (\text{Diag}(w_i^2)x_0)|^2), i = 1 \dots r$. We then obtain the one bit CDP by quantizing pairs of CDPs. In our experiment we have $n = 256 \times 256$, $r = 10 \lfloor \log(n) \rfloor$.

In Figure 11(b), we show the output of Algorithm 1 given the one bit CDP collected as mentioned previously. We see that most of the missing details in Figure 11(a) are recovered. Hence one bit phase retrieval enables super-resolution and blind deconvolution as it is agnostic to the nature of the blur.



(a) Image convolved with an averaging filter of size 8×8 .

(b) Recovered image from One Bit CDP .

Figure 11: Super-Resolution and Blind Deconvolution via Phase Retrieval from One Bit CDP.

6.2.4 One Bit Phase Retrieval and Alternating Minimization

In this section we test the alternating minimization Algorithm 3 initialized with One Bit Phase Retrieval (Algorithm 1), in the noiseless and the Poisson noise model of equation (19). To emphasize the effect of the initialization we set the number of iterations t_0 in Algorithm 3 to a relatively small number. In our experiments we set $t_0 = 50$, and $r = 4$. We test our algorithms with Complex Gaussian masks and Bernoulli masks.

Gaussian masks. We start by the recovery for a noiseless acquisition of the CDP, the recovered image with alternating minimization initialized with one bit phase retrieval is given in Figure 12(a) and is indistinguishable from the original. The average SNR on the three color channels is 101.2248 dB. When the CDP are contaminated with a poisson noise (In Equation (19) we set $\eta = 0.1$), Alternating minimization initialized with one bit phase retrieval succeeds and produces a solution with an average SNR on the three color channels of 95.625 dB. The recovered image in this setting is shown Figure 12(b).

Bernoulli masks. We repeat the same experiment with bernoulli masks , i.e each entry of the mask is a bernoulli random variable with parameter $p = 0.8$. The Recovered image in the noiseless is given in Figure 13(a), the average SNR is 97 dB. In the poisson noise setting the recovered image is given in Figure 13(b), the average SNR is 95.0769 dB. We see that the quality for this fixed number of masks and iterations is lower than the Gaussian case.



(a) Recovered Image with AM initialized with the *1bitPhase* solution, for a noiseless acquisition of CDP.



(b) Recovered Image with AM initialized with the *1bitPhase* solution, for an acquisition where the CDP are contaminated with a Poisson Noise.

Figure 12: Alternating Minimization and One Bit Phase Retrieval from Gaussian masks.



(a) Recovered Image with AM initialized with the *1bitPhase* solution, for a noiseless acquisition of CDP.



(b) Recovered Image with AM initialized with the *1bitPhase* solution, for an acquisition where the CDP are contaminated with a Poisson Noise.

Figure 13: Alternating Minimization and One Bit Phase Retrieval from Bernoulli masks.

7 Acknowledgements

I am thankful for fruitful discussions with Tomaso Poggio, Lorenzo Rosasco and Gadi Geiger. I would like also to thank Gordon Wetzstein for pointing out reference [ZHY13] and for inspiring discussions on Super-Resolution and applications in microscopy. I am also thankful to Chiyuan Zhang for providing his drawing of Stata center.

8 Proofs

In this section we give the proofs of Proposition 2, Lemma 1 and Proposition 3. We start with the following observation:

Lemma 3. *Let $y \in \mathbb{C}^n$, and $M \in \mathbb{C}^{n \times n}$, we have the following equality:*

$$\langle y, \text{diag}(M) \rangle = \text{Tr}(\text{Diag}(y)^* M). \quad (40)$$

We need this result for $y \in \mathbb{R}^n$:

$$\langle y, \text{diag}(M) \rangle = \text{Tr}(\text{Diag}(y)M). \quad (41)$$

Let $v = F^* \text{Diag}(w^*)x$ and $u = F^* \text{Diag}(w^*)x_0$. The proof of proposition 1 follows from Lemmas 4 and 5:

Lemma 4. *The modulus vector can be rewritten in the following way:*

$$|F \text{Diag}(w)x|^2 = \text{diag} \{ F^* \text{Diag}(w^*)x x^* \text{Diag}(w)F \} = \text{diag}(v v^*).$$

Lemma 5. *The following equation holds :*

$$\langle y, |F \text{Diag}(w)x|^2 \rangle = x^* \text{Diag}(w)F \text{Diag}(y)F^* \text{Diag}(w^*)x.$$

Proof of Proposition 1. By Lemma 5

$$\begin{aligned} \mathcal{E}^{x_0}(x) &= \mathbb{E}(\langle y, |F \text{Diag}(w^1)x|^2 - |F \text{Diag}(w^2)x|^2 \rangle) \\ &= x^* C x. \end{aligned}$$

where $C = \mathbb{E}(\text{Diag}(w^1)F \text{Diag}(y)F^* \text{Diag}(w^{1,*}) - \text{Diag}(w^2)F \text{Diag}(y)F^* \text{Diag}(w^{2,*}))$. □

Proof of Lemma 4.

$$|F \text{Diag}(w)x|^2[i] = \sum_j F_{ij} w_j x_j \sum_k \bar{F}_{ik} \bar{w}_k \bar{x}_k = \sum_{jk} F_{ij} \bar{F}_{ik} \bar{w}_k w_j x_j \bar{x}_k. \quad (42)$$

On the other hand:

$$e_i^* F^* \text{Diag}(w^*)x x^* \text{Diag}(w)F e_i = [\bar{F}_{i1} \dots \bar{F}_{in}] \mathcal{W} [F_{i1} \dots F_{in}]', \quad (43)$$

where $\mathcal{W}_{jk} = w_j \bar{w}_k x_j \bar{x}_k$. Hence :

$$e_i^* F^* \text{Diag}(w^*)x x^* \text{Diag}(w)F e_i = \sum_{jk} F_{ij} \bar{F}_{ik} \bar{w}_k w_j x_j \bar{x}_k. \quad (44)$$

The lemma is proved. □

Proof of Lemma 5. Using Lemma 3 and Lemma 4, we have:

$$\begin{aligned}
\langle y, |F\text{Diag}(w)x|^2 \rangle &= \langle y, \text{diag}\{F^*\text{Diag}(w^*)xx^*\text{Diag}(w)F\} \rangle \\
&= \text{Tr}(\text{Diag}(y)F^*\text{Diag}(w^*)xx^*\text{Diag}(w)F) \\
&= \text{Tr}(\text{Diag}(w)F\text{Diag}(y)F^*\text{Diag}(w^*)xx^*) \\
&= x^*\text{Diag}(w)F\text{Diag}(y)F^*\text{Diag}(w^*)x.
\end{aligned}$$

□

Proof of Proposition 2. i-Let $v = F^*\text{Diag}(w^*)x$ and $u = F^*\text{Diag}(w^*)x_0$, v_i and $u_i \sim \mathcal{CN}(0, \frac{1}{n})$, $i = 1 \dots n$. u and v are gaussian vectors with dependent coordinates. The expectation of dot product $\langle u, v \rangle$ is given in the following:

$$\mathbb{E}(\langle u, v \rangle) = \mathbb{E}(x_0^*\text{Diag}(w)FF^*\text{Diag}(w^*)x) = x_0^*\mathbb{E}(\text{Diag}(|w|^2))x = \langle x_0, x \rangle.$$

since $FF^* = I$, and $\mathbb{E}(\text{Diag}(|w|^2)) = I_n$.

Hence $\mathbb{E}(\|u\|^2) = \mathbb{E}(\|v\|^2) = 1$, since x and x_0 are unitary.

There exists a complex Gaussian random vector r , such that each $r_i \sim \mathcal{CN}(0, \frac{1}{n})$ and r_i is independent of u_i , $i = 1 \dots n$ and:

$$v = \langle x_0, x \rangle u + \sqrt{1 - |\langle x_0, x \rangle|^2} r$$

Let $v_1 = F^*\text{Diag}(w^{1,*})x$, $u_1 = F^*\text{Diag}(w^{1,*})x_0$, and $v_2 = F^*\text{Diag}(w^{2,*})x$, $u_2 = F^*\text{Diag}(w^{2,*})x_0$. By lemma 4 we have:

$$\begin{aligned}
\mathcal{E}^{x_0}(x) &= \mathbb{E}(\langle y, |F\text{Diag}(w^1)x|^2 - |F\text{Diag}(w^2)x|^2 \rangle) \\
&= \mathbb{E}(\langle y, \text{diag}(v_1v_1^* - v_2v_2^*) \rangle)
\end{aligned}$$

On the other hand:

$$\begin{aligned}
vv^* &= (\langle x_0, x \rangle u + \sqrt{1 - |\langle x_0, x \rangle|^2} r)(\overline{\langle x_0, x \rangle} u^* + \sqrt{1 - |\langle x_0, x \rangle|^2} r^*) \\
&= |\langle x_0, x \rangle|^2 uu^* + (1 - |\langle x_0, x \rangle|^2) rr^* + 2\sqrt{1 - |\langle x_0, x \rangle|^2} \text{Re}(\langle x_0, x \rangle ur^*)
\end{aligned}$$

Therefore:

$$\begin{aligned}
\text{diag}(v_1v_1^* - v_2v_2^*) &= |\langle x_0, x \rangle|^2 \text{diag}(u_1u_1^* - u_2u_2^*) + (1 - |\langle x_0, x \rangle|^2) \text{diag}(r_1r_1^* - r_2r_2^*) \\
&\quad + 2\sqrt{1 - |\langle x_0, x \rangle|^2} \text{diag}(\text{Re}(\langle x_0, x \rangle (u_1r_1^* - u_2r_2^*))) \\
&= |\langle x_0, x \rangle|^2 (|F\text{Diag}(w^1)x_0|^2 - |F\text{Diag}(w^2)x_0|^2) + (1 - |\langle x_0, x \rangle|^2) \text{diag}(r_1r_1^* - r_2r_2^*) \\
&\quad + 2\sqrt{1 - |\langle x_0, x \rangle|^2} \text{diag}(\text{Re}(\langle x_0, x \rangle (u_1r_1^* - u_2r_2^*))).
\end{aligned}$$

Therefore, taking the expectation we have:

$$\mathcal{E}^{x_0}(x) = |\langle x_0, x \rangle|^2 \mathbb{E}(\langle y, |F\text{Diag}(w^1)x_0|^2 - |F\text{Diag}(w^2)x_0|^2 \rangle)$$

since $\mathbb{E}_{u_1, u_2} \langle y, \mathbb{E}_{r_1, r_2}(\text{diag}(r_1r_1^* - r_2r_2^*)|u_1, u_2) \rangle = 0$,

and $\mathbb{E}_{u_1, u_2} (\langle y, \mathbb{E}_{r_1, r_2}(\text{diag}(\text{Re}((u_1r_1^* - u_2r_2^*)))|u_1, u_2) \rangle) = 0$.

Let

$$\lambda = \mathbb{E}(\langle y, |F\text{Diag}(w^1)x_0|^2 - |F\text{Diag}(w^2)x_0|^2 \rangle).$$

Let $\tilde{E}_i^1 = |\sum_{j=1}^n F_{ij} w_j x_{0,j}|^2$, since w_j is complex Gaussian, $\sum_{j=1}^n F_{ij} w_j x_{0,j}$ is $\mathcal{CN}(0, \frac{1}{n})$, therefore \tilde{E}_i^1 is exponential with mean $\frac{1}{n}$ (since $|F_{ij}|^2 = 1$). Let E_i^1 be an exponential with mean 1. $\tilde{E}_i^1 = \frac{1}{n} E_i^1$. It follows that:

$$\begin{aligned}\lambda &= \mathbb{E}(\langle y, |FDiag(w^1)x_0|^2 - |FDiag(w^2)x_0|^2 \rangle) \\ &= \frac{1}{n} \sum_{i=1}^n \mathbb{E}(y_i(E_i^1 - E_i^2)) \\ &= \frac{1}{n} n \mathbb{E}(y(E^1 - E^2)) \\ &= \mathbb{E}(y(E^1 - E^2))\end{aligned}$$

Where λ is defined for different models in Lemma 2. □

Remark 1. Similar results hold if we use instead of the DFT F any unitary matrix U . The value of λ would depend on $|U_{ij}|^2$.

Proof of Lemma 2. i. Noiseless:

$$\lambda = \mathbb{E}(\text{sign}(E_1 - E_2)(E_1 - E_2)) = \mathbb{E}(|E_1 - E_2|) = 1, \text{ since } E_1 - E_2 \sim \text{Exp}(1).$$

ii. *Noisy:*

Let $y = \text{sign}((E_1 + \nu_1) - (E_2 + \nu_2))$. Let $L = E_1 - E_2$, L follows a Laplace distribution with mean 0 and scale parameter 1:

$$L \sim \text{Laplace}(0, 1).$$

Let $N = \nu_1 - \nu_2$, N follows a Laplace distribution, $N \sim \text{Laplace}(0, \frac{1}{\gamma})$. It follows that:

$$\begin{aligned}\lambda &= \mathbb{E}_{L,N}(\text{sign}(L + N)L) \\ &= \mathbb{E}_L((1 - 2\mathbb{P}_N(N \leq -L))L) \\ &= \mathbb{E}_L((1 - 2F_N(-L))L) \\ &= \mathbb{E}_L\left\{\left(1 - 2\left(\frac{1}{2} + \frac{1}{2}\text{sign}(-L)(1 - \exp(-\gamma|L|))\right)\right)L\right\} \\ &= \mathbb{E}_L(\text{sign}(L)(1 - \exp(-\gamma|L|))L) \\ &= \mathbb{E}_L|L|(1 - \exp(-\gamma|L|)) \\ &= 1 - \int_0^{+\infty} z \exp(-\gamma z) \exp(-z) dz \\ &= 1 - \frac{1}{(1 + \gamma)^2} > 0.\end{aligned}$$

Let $\sigma = \frac{1}{\gamma^2}$ be the variance of the exponential noise. We conclude that:

$$\lambda = \frac{1 + 2\sqrt{\sigma}}{(1 + \sqrt{\sigma})^2}.$$

iii. *Distortion:*

$$\begin{aligned}y &= \text{sign}(\tanh(\alpha E_1) - \tanh(\alpha E_2)) \\ &= \text{sign}(\tanh(\alpha(E_1 - E_2))) (1 - \tanh(\alpha E_1) \tanh(\alpha E_2)) \\ &= \text{sign}(\tanh(\alpha(E_1 - E_2))). \text{sign}(1 - \tanh(\alpha E_1) \tanh(\alpha E_2)) \\ &= \text{sign}(E_1 - E_2) \text{sign}(1 - \tanh(\alpha E_1) \tanh(\alpha E_2))\end{aligned}$$

$$\lambda = \mathbb{E}(y(E_1 - E_2)) = \mathbb{E}(\text{sign}(1 - \tanh(\alpha E_1) \tanh(\alpha E_2)) |E_1 - E_2|). \quad \square$$

Proof of Lemma 1. For $x \in \mathbb{C}^n, \|x\| = 1$, let $\mathcal{E}^{x_0}(x) = x^* C x$, and $\hat{\mathcal{E}}^{x_0}(x) = x^* \hat{C}_r x$.

$$\mathcal{E}^{x_0}(x_0) - \mathcal{E}^{x_0}(x) = \lambda - \lambda |\langle x_0, x \rangle|^2 = \frac{\lambda}{2} \|x x^* - x_0 x_0^*\|_F^2.$$

Let $\hat{x}_r = \arg \max_{x, \|x\|=1} \hat{\mathcal{E}}^{x_0}(x)$, we have:

$$\mathcal{E}^{x_0}(x_0) - \mathcal{E}^{x_0}(\hat{x}_r) = \mathcal{E}^{x_0}(x_0) - \hat{\mathcal{E}}^{x_0}(x_0) + \hat{\mathcal{E}}^{x_0}(x_0) - \hat{\mathcal{E}}^{x_0}(\hat{x}_r) + \hat{\mathcal{E}}^{x_0}(\hat{x}_r) - \mathcal{E}^{x_0}(\hat{x}_r).$$

Noticing that the term $\hat{\mathcal{E}}^{x_0}(x_0) - \hat{\mathcal{E}}^{x_0}(\hat{x}_r)$ is non-positive in light of the definition of \hat{x}_r , we have finally: $\mathcal{E}^{x_0}(x_0) - \mathcal{E}^{x_0}(\hat{x}_r) \leq 2 \sup_{x, \|x\|=1} \hat{\mathcal{E}}^{x_0}(x) - \mathcal{E}^{x_0}(x) = 2 \left\| \hat{C}_r - C \right\|$. Finally:

$$\frac{\lambda}{2} \|\hat{x}_r \hat{x}_r^* - x_0 x_0^*\|_F^2 = \mathcal{E}^{x_0}(x_0) - \mathcal{E}^{x_0}(\hat{x}_r) \leq 2 \sup_{x, \|x\|=1} \hat{\mathcal{E}}^{x_0}(x) - \mathcal{E}^{x_0}(x) = 2 \left\| \hat{C}_r - C \right\| \quad (45)$$

□

Proof of Proposition 3. It follows that:

$$\mathbb{E}(\hat{C}_r) = \lambda x_0 x_0^*$$

Where $\hat{C}_r = \frac{1}{r} \sum_{i=1}^r A_i$ where $A_i = \text{Diag}(w_i^1) F \text{Diag}(y_i) F^* \text{Diag}(w_i^{1,*}) - \text{Diag}(w_i^2) F \text{Diag}(y_i) F^* \text{Diag}(w_i^{2,*})$ $i = 1 \dots r$.

By Lemma 1, it is now clear that the sample complexity is governed by the concentration of \hat{C}_r around its mean. Let $E_\beta = \{w \in \mathbb{C}^n, |w_j^1|^2 \leq 2\beta \log(n) \text{ and } |w_j^2|^2 \leq 2\beta \log(n), j = 1 \dots n\}$. Let $(w_i^1, w_i^2), i = 1 \dots r$, be $2r$ independent iid $\mathcal{CN}(0, I_n)$. Define $(\tilde{w}_i^1, \tilde{w}_i^2) = (w_i^1, w_i^2)$ if $(w_i^1, w_i^2) \in E_\beta$ and $(\tilde{w}_i^1, \tilde{w}_i^2) = (0, 0)$ elsewhere.

Define $\tilde{C}_r = \frac{1}{r} \sum_{i=1}^r \tilde{A}_i$, where

$$\tilde{A}_i = \text{Diag}(\tilde{w}_i^1) F \text{Diag}(\tilde{y}_i) F^* \text{Diag}(\tilde{w}_i^{1,*}) - \text{Diag}(\tilde{w}_i^2) F \text{Diag}(\tilde{y}_i) F^* \text{Diag}(\tilde{w}_i^{2,*}),$$

and let $\tilde{C} = \mathbb{E} \tilde{C}_r$. By the triangular inequality we have:

$$\left\| \hat{C}_r - C \right\| \leq \left\| \hat{C}_r - \tilde{C}_r \right\| + \left\| \tilde{C}_r - \tilde{C} \right\| + \left\| \tilde{C} - C \right\| \quad (46)$$

Bounding $\left\| \hat{C}_r - \tilde{C}_r \right\|$:

Note that $\left\| \hat{C}_r - \tilde{C}_r \right\| = 0$, if for all $i = 1 \dots r$, $(w_i^1, w_i^2) \in E_\beta$. Let us get a bound on the probability of that event. Note that: $\mathbb{P}(|w_i|^2 > 2\beta \log(n)) \leq 2n^{-\beta}$. To avoid cumbersome notations when we use index i , w_i refers to a modulation in \mathbb{C}^n , $i = 1 \dots r$, and when we use index j w_j refers to the j -th component of $w \in \mathbb{C}^n, j = 1 \dots n$.

$$\begin{aligned} \mathbb{P} \{ \exists i \in \{1 \dots r\} \text{ such that } (w_i^1, w_i^2) \notin E_\beta \} &\leq r \mathbb{P} \{ (w^1, w^2) \notin E_\beta \} \\ &= r \mathbb{P} \{ \exists j \text{ such that } |w_j^1|^2 > 2\beta \log(n) \text{ Or } |w_j^2|^2 > 2\beta \log(n) \} \\ &\leq \frac{4rn}{n^\beta}. \end{aligned}$$

It follows that:

$$\left\| \hat{C}_r - \tilde{C}_r \right\| = 0 \text{ with probability at least } 1 - \frac{4r}{n^{\beta-1}}. \quad (47)$$

Bounding $\left\| \tilde{C}_r - \tilde{C} \right\|$:

Let

$$\tilde{X}_i = \tilde{A}_i - \mathbb{E}(\tilde{A}_i),$$

$\mathbb{E}(\tilde{X}_i) = 0$. Note that

$$\left\| \tilde{C}_r - \tilde{C} \right\| = \frac{1}{r} \left\| \sum_{i=1}^r \tilde{X}_i \right\|$$

Let us get a bound on $\|\tilde{X}_i\|$. Note that $\|\mathbb{E}(\tilde{A}_i)\| \leq \lambda$. To simplify the notation we will omit in the following the indices.

$$\left\| \tilde{A} \right\| = \sup_{x, \|x\|=1} \langle \tilde{y}, |F \text{Diag}(\tilde{w}^1)x|^2 - |F \text{Diag}(\tilde{w}^2)x|^2 \rangle$$

Recall that $v = F^* \text{Diag}(\tilde{w}^*)x$. Note that: $|F \text{Diag}(\tilde{w})x|^2 = \text{diag} \{ F^* \text{Diag}(\tilde{w}^*)xx^* \text{Diag}(\tilde{w})F \} = \text{diag}(vv^*)$.

By holder inequality we have:

$$\begin{aligned} \langle \tilde{y}, |F \text{Diag}(\tilde{w}^1)x|^2 - |F \text{Diag}(\tilde{w}^2)x|^2 \rangle &= \langle \tilde{y}, \text{diag}(v^1 v^{1,*}) - \text{diag}(v^2 v^{2,*}) \rangle \\ &\leq \|\tilde{y}\|_\infty \left\| \text{diag}(v^1 v^{1,*}) - \text{diag}(v^2 v^{2,*}) \right\|_{\ell_1}. \end{aligned}$$

Since \tilde{y} is binary $\|\tilde{y}\|_\infty = 1$. By the triangular inequality:

$$\left\| \text{diag}(v^1 v^{1,*}) - \text{diag}(v^2 v^{2,*}) \right\|_{\ell_1} \leq \left\| \text{diag}(v^1 v^{1,*}) \right\|_{\ell_1} + \left\| \text{diag}(v^2 v^{2,*}) \right\|_{\ell_1}.$$

$$\begin{aligned} \left\| \text{diag}(vv^*) \right\|_{\ell_1} &= \left\| |F \text{Diag}(w)x|^2 \right\|_{\ell_1} = \left\| \text{diag} \{ F^* \text{Diag}(\tilde{w}^*)xx^* \text{Diag}(\tilde{w})F \} \right\|_{\ell_1} \\ &= \text{Tr}(F^* \text{Diag}(\tilde{w}^*)xx^* \text{Diag}(\tilde{w})F) \\ &= \text{Tr}(\text{Diag}(\tilde{w})FF^* \text{Diag}(\tilde{w}^*)xx^*) \\ &= \text{Tr}(\text{Diag}(|\tilde{w}|^2)xx^*) \\ &\leq \left\| \text{Diag}(|\tilde{w}|^2) \right\| \|x\|^2. \end{aligned}$$

We are now left with Bounding:

$$\begin{aligned} \sup_{x, \|x\|=1} \left(\left\| \text{Diag}(|\tilde{w}^1|^2) \right\| + \left\| \text{Diag}(|\tilde{w}^2|^2) \right\| \right) \|x\|^2 &= \left(\left\| \text{Diag}(|\tilde{w}^1|^2) \right\| + \left\| \text{Diag}(|\tilde{w}^2|^2) \right\| \right) \\ &= \max_{j=1 \dots n} |\tilde{w}_j^1|^2 + \max_{j=1 \dots n} |\tilde{w}_j^2|^2 \end{aligned} \quad (48)$$

By definition of $(\tilde{w}^1, \tilde{w}^2)$ we conclude that :

$$\|\tilde{A}\| \leq 4\beta \log(n). \quad (49)$$

It follows that

$$\|\tilde{X}_i\| \leq 4\beta \log(n) + \lambda \leq 5\beta \log(n) := \Delta.$$

Theorem 2 (Hoeffding Matrix Inequality [Tro12]). *Let $X_i, i = 1 \dots r$ be a sequence of independent random $n \times n$ self adjoint matrices. Assume that each random matrix obeys:*

$$\mathbb{E}(X_i) = 0 \quad \text{and} \quad \|X_i\| \leq \Delta \quad \text{almost surely.}$$

Then for all $t \geq 0$,

$$\mathbb{P} \left\{ \frac{1}{r} \left\| \sum_{i=1}^r X_i \right\| \geq t \right\} \leq 2n \exp \left(-\frac{rt^2}{8\Delta^2} \right).$$

In other words:

$$\text{For } r \geq \frac{t^2}{\epsilon^2} \Delta^2 \log(n), \quad \frac{1}{r} \left\| \sum_{i=1}^r X_i \right\| \leq \epsilon \text{ with probability at least } 1 - n^{-t^2}.$$

We are now ready to apply the Hoeffding Matrix inequality:

$$\text{For } r \geq c \frac{t^2}{\epsilon^2} \beta^2 \log^3 n, \quad \frac{1}{r} \left\| \sum_{i=1}^r \tilde{X}_i \right\| \leq \epsilon \text{ with probability at least } 1 - n^{-t^2}.$$

It follows that:

$$\text{For } \left\| \tilde{C}_r - \tilde{C} \right\| \leq ct\beta \sqrt{\frac{\log^3 n}{r}} \text{ with probability at least } 1 - n^{-t^2}. \quad (50)$$

Bounding $\left\| \tilde{C} - C \right\|$:

By Jensen inequality followed by Cauchy Sharwz inequality we have:

$$\begin{aligned} \left\| \tilde{C} - C \right\| &= \left\| \mathbb{E} \left(\mathbf{1}_{w^1, w^2 \notin E_\beta} A \right) \right\| \\ &\leq \mathbb{E} \mathbf{1}_{w^1, w^2 \notin E_\beta} \|A\| \\ &\leq \sqrt{\mathbb{E}(\mathbf{1}_{w^1, w^2 \notin E_\beta})} \sqrt{E(\|A\|^2)} \\ &\leq \sqrt{\mathbb{P}(E_\beta^c)} \sqrt{\mathbb{E}(\max_{j=1\dots n} |w_j^1|^2 + \max_{j=1\dots n} |w_j^2|^2)^2}. \end{aligned}$$

The last inequality follows from equation (48).

$$\|A\|^2 \leq (\max_{j=1\dots n} |w_j^1|^2)^2 + (\max_{j=1\dots n} |w_j^2|^2)^2 + 2 \max_{j=1\dots n} |w_j^1|^2 \max_{j=1\dots n} |w_j^2|^2. \quad (51)$$

Let $Z = \max_{j=1\dots n} E_j$, $E_j \sim \text{Exp}(1)$ iid, therefore:

$$\mathbb{E}(\|A\|^2) \leq 2(E(Z^2) + (E(Z))^2) = 2(\text{Var}(Z)) + 2(E(Z))^2. \quad (52)$$

Lemma 6 (Maximum of Exponential [BT12]). *Let $Z = \max_{j=1\dots n} E_j$, $E_j \sim \text{Exp}(1)$ iid, therefore: $\text{Var}(Z) \leq 2$ $\mathbb{E}(Z) = \sum_{i=1}^n \frac{1}{i} \leq \log(n)$.*

For sufficiently large n , there exists a constant c such that:

$$\mathbb{E}(\|A\|^2) \leq 2(E(Z^2) + (E(Z))^2) = 2(2 + 2(\log^2(n))) = 4(1 + \log^2(n)) \leq c^2 \log^2(n). \quad (53)$$

Note that $\mathbb{P}(E_\beta^c) \leq \frac{4n}{n^\beta}$. Therefore:

$$\left\| \tilde{C} - C \right\| \leq \frac{2c}{n^{(\beta-1)/2}} \log(n). \quad (54)$$

Putting all together:

Putting together equations (46),(47),(50) and (54) we have finally with probability at least $1 - n^{-t^2} - \frac{4r}{n^{\beta-1}}$:

$$\|\hat{C}_r - C\| \leq c\beta t \sqrt{\frac{\log^3 n}{r} + \frac{2c}{n^{(\beta-1)/2}} \log(n)}. \quad (55)$$

Setting $t = \sqrt{2}, \beta = 4$ we get with probability $1 - O(n^{-2})$,

$$\|\hat{C}_r - C\| \leq 4\sqrt{2}c \sqrt{\frac{\log^3 n}{r} + \frac{2c}{n^{3/2}} \log(n)}. \quad (56)$$

It follows that there exists a numeric constant c such that:

$$\text{For } r \geq c \frac{\log^3 n}{\epsilon^2} \quad \|\hat{C}_r - C\| \leq \epsilon, \text{ with probability at least } 1 - O(n^{-2}). \quad (57)$$

Finally by equation (45) we conclude that:

$$\text{For } r \geq c \frac{\log^3 n}{\epsilon^2} \quad \frac{1}{2} \|\hat{x}_r \hat{x}_r^* - x_0 x_0^*\|_F^2 \leq \frac{\epsilon}{\lambda}, \text{ with probability at least } 1 - O(n^{-2}). \quad (58)$$

In other words for another numeric constant c we have:

$$\text{For } r \geq c \frac{\log^3 n}{\epsilon^2 \lambda^2} \quad \|\hat{x}_r \hat{x}_r^* - x_0 x_0^*\|_F^2 \leq \epsilon, \text{ with probability at least } 1 - O(n^{-2}). \quad (59)$$

References

- [ABFM12] B. Alexeev, A. S. Bandeira, M. Fickus, and D. G. Mixon. Phase retrieval with polarization. *arXiv preprint arXiv:1210.7752*, 12(4):389–434, 2012.
- [ASBM13] Y. Chen A. S. Bandeira and D. G. Mixon. Phase retrieval from power spectra of masked signals. *arXiv preprint arXiv:1303.4458*, 2013.
- [BDP⁺07] O. Bunk, A. Diaz, F. Pfeiffer, C. David, B. Schmitt, D.K. Satapathy, and JF Veen. Diffractive imaging for periodic samples: retrieving one-dimensional concentration profiles across microfluidic channels. *Acta Crystallographica Section A: Foundations of Crystallography*, 63(4):306314, 2007.
- [BT12] S. Boucheron and M. Thomas. Concentration inequalities for order statistics. *Electronic communication in probability*, 2012.
- [CL12] E. J. Candes and X. Li. Solving quadratic equations via phaselift when there are about as many equations as unknowns. *To appear in Foundations of Computational Mathematics.*, 2012.
- [CLM13] E. Candes, X. Li, and M.Soltanolkotab. Phase retrieval from coded diffraction patterns. *arxiv*, 2013.
- [CSV11] E. J. Candes, T. Strohmer, and V. Voroninski. Phaselift : exact and stable signal recovery from magnitude measurements via convex programming. *To appear in Communications in Pure and Applied Mathematics*, 2011.
- [DH12] L. Demanet and P. Hand. Stable optimizationless recovery from phaseless linear measurements. *arXiv:1208.1803*, 2012.

- [FGC12] C. Fernandez-Granda and E. J. Candes. Towards a mathematical theory of super-resolution. *To appear in Communications on Pure and Applied Mathematics*, 2012.
- [Fie82] J.R. Fienup. Phase retrieval algorithms: a comparison. *Applied optics*, 21(15):2758-2769, 1982.
- [Fri66] D.L. Fried. Optical resolution through a randomly inhomogeneous medium for very long and very short exposures. *Journal of physics, J. Opt. Soc. Am.* 56, 1372-1379, 1966.
- [GL84] D. Griffin and J. Lim. Signal estimation from modified short-time fourier transform. *Acoustics, Speech and Signal Processing, IEEE Transactions on*, 32(2):236-243, 1984.
- [GS72] R. Gerchberg and W. Saxton. A practical algorithm for the determination of phase from image and diffraction plane pictures. *Optik*, 35:237-246, 1972.
- [Gus00] M. G. L. Gustafsson. Surpassing the lateral resolution limit by a factor of two using structured illumination microscopy. *Journal of Microscopy*, 198, Pt 2, May 2000, pp. 8287, 2000.
- [Har93] R.W. Harrison. Phase problem in crystallography. *JOSA A*, 10(5):1046-1055, 1993.
- [HKH⁺13] M.J. Humphry, B. Kraus, A.C. Hurst, A.M. Maiden, and J.M. Rodenburg. Ptychographic electron microscopy using high-angle dark-field scattering for sub-nanometre resolution imaging. *Nature*, 2013.
- [Lea08] Y. J. Liu and et al. Phase retrieval in x-ray imaging based on using structured illumination. *Phys. Rev. A*, 78:023817, 2008.
- [LT91] M. Ledoux and M. Talagrand. Probability in banach spaces: isoperimetry and processes. *Springer-Verlag*, 1991.
- [Mis73] D.L. Misell. A method for the solution of the phase problem in electron microscopy. *Journal of physics*, 1973.
- [MISE08] J. Miao, T. Ishikawa, Q. Shen, and T. Earnest. Extending x-ray crystallography to allow the imaging of noncrystalline materials, cells, and single protein complexes. *Annu. Rev. Phys. Chem.*, 59:387-410, 2008.
- [MR13] Y. Mroueh and L. Rosasco. Quantization and greed are good: One bit phase retrieval, robustness and greedy refinements. *submitted*, 2013.
- [NJS13] Praneeth Netrapalli, Prateek Jain, and Sujay Sanghavi. Phase retrieval using alternating minimization. *NIPS*, 2013.
- [Rod08] J.M. Rodenburg. Ptychography and related diffractive imaging methods. *Advances in Imaging and Electron Physics*, vol. 150, 150:87-184, 2008.
- [Tro12] J. A. Tropp. User-friendly tail bounds for sums of random matrices. *Foundations of Computational Mathematics*, 12(4):389-434, 2012.
- [YZ97] I. Yamaguchi and T. Zhang. Phase-shifting digital holography. *Opt. Lett.* 22, 1268-1270, 1997.
- [ZHY13] G. Zheng, R. Horstmeyer, and C. Yang. Wide-field, high-resolution fourier ptychographic microscopy. *Nature Photonics*, doi:10.1038/nphoton.2013.187, 2013.